NAVAL POSTGRADUATE SCHOOL
Monterey, California

THESIS

FEASIBILITY OF PARAMETRIC EXCITATION OF ACOUSTIC RESONATORS

by

Larry P. Varnadore

June 2001

Thesis Advisor: Bruce C. Denardo
Second Reader: Thomas J. Hofler

Approved for public release; distribution is unlimited

REPORT DOCUMENTATION PAGE			Form Approved OMB No. 0704-0188
Public reporting burden for this collection of information is estimated to average 1 hour per response, including the time for reviewing instruction, searching existing data sources, gathering and maintaining the data needed, and completing and reviewing the collection of information. Send comments regarding this burden estimate or any other aspect of this collection of information, including suggestions for reducing this burden, to Washington headquarters Services, Directorate for Information Operations and Reports, 1215 Jefferson Davis Highway, Suite 1204, Arlington, VA 22202-4302, and to the Office of Management and Budget, Paperwork Reduction Project (0704-0188) Washington DC 20503.			
1. AGENCY USE ONLY *(Leave blank)*	**2. REPORT DATE** June 2001	**3. REPORT TYPE AND DATES COVERED** Master's Thesis	
4. TITLE AND SUBTITLE: Title (Mix case letters) Feasibility of Parametric Excitation of Acoustic Resonators			**5. FUNDING NUMBERS**
6. AUTHOR(S) Varnadore, Larry P.			
7. PERFORMING ORGANIZATION NAME(S) AND ADDRESS(ES) Naval Postgraduate School Monterey, CA 93943-5000			**8. PERFORMING ORGANIZATION REPORT NUMBER**
9. SPONSORING / MONITORING AGENCY NAME(S) AND ADDRESS(ES) N/A			**10. SPONSORING / MONITORING AGENCY REPORT NUMBER**
11. SUPPLEMENTARY NOTES The views expressed in this thesis are those of the author and do not reflect the official policy or position of the Department of Defense or the U.S. Government.			
12a. DISTRIBUTION / AVAILABILITY STATEMENT Approved for public release; distribution is unlimited.			**12b. DISTRIBUTION CODE**

ABSTRACT ***(maximum 200 words)***

This thesis examines the feasibility of parametrically exciting a mode of an acoustic resonator. Such excitation may result in substantially larger amplitudes than by direct excitation, and would thus be useful in acoustic devices that require high-amplitude standing waves. Parametric excitation of a mode occurs if the natural frequency is modulated at twice its value, and if the drive amplitude is above a threshold value due to dissipation. It is theoretically shown to be possible to excite the fundamental longitudinal mode of a pipe of any length filled with sulfur hexafluoride if the length is modulated with an Electrovoice EVX-150A driver. For carbon dioxide, excitation is predicted to occur if the pipe is longer than 1.2 meters. Also investigated is parametric excitation of the fundamental radial mode of a cylindrical cavity by modulating the height and thus the temperature. In this case, no driver was found to be capable of exceeding the threshold, regardless of the gas. Use of an electromagnetic wave source to modulate the temperature was also considered as a means of parametrically exciting the fundamental radial mode. Preliminary investigations show that sufficient heat conduction cannot occur over an acoustic cycle, indicating that this method is infeasible.

14. SUBJECT TERMS Parametric Excitation, Acoustic Resonators, Acoustics			**15. NUMBER OF PAGES** 126
			16. PRICE CODE
17. SECURITY CLASSIFICATION OF REPORT Unclassified	**18. SECURITY CLASSIFICATION OF THIS PAGE** Unclassified	**19. SECURITY CLASSIFICATION OF ABSTRACT** Unclassified	**20. LIMITATION OF ABSTRACT** UL

NSN 7540-01-280-5500

Standard Form 298 (Rev. 2-89)
Prescribed by ANSI Std. 239-18

THIS PAGE INTENTIONALLY LEFT BLANK

Approved for public release; distribution is unlimited

FEASIBILITY OF PARAMETRIC EXCITATION OF ACOUSTIC RESONATORS

Larry P. Varnadore
Lieutenant, United States Navy
B.S., Auburn University, 1993

Submitted in partial fulfillment of the
requirements for the degree of

MASTER OF SCIENCE IN APPLIED PHYSICS

from the

NAVAL POSTGRADUATE SCHOOL
June 2001

Author: 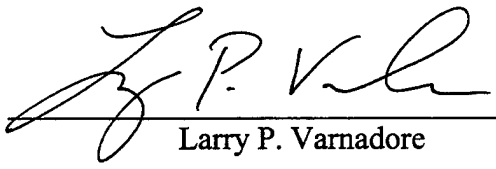
Larry P. Varnadore

Approved by: 
Bruce C. Denardo, Thesis Advisor

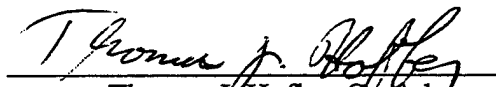
Thomas J. Hofler, Co-Advisor

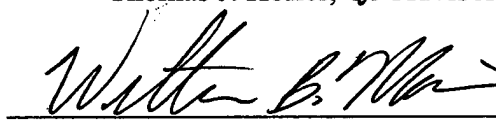
William B. Maier II, Chair
Department of Physics

THIS PAGE INTENTIONALLY LEFT BLANK

ABSTRACT

This thesis examines the feasibility of parametrically exciting a mode of an acoustic resonator. Such excitation may result in substantially larger amplitudes than by direct excitation, and would thus be useful in acoustic devices that require high-amplitude standing waves. Parametric excitation of a mode occurs if the natural frequency is modulated at twice its value, and if the drive amplitude is above a threshold value due to dissipation. It is theoretically shown to be possible to excite the fundamental longitudinal mode of a pipe of any length filled with sulfur hexafluoride if the length is modulated with an Electrovoice EVX-150A driver. For carbon dioxide, excitation is predicted to occur if the pipe is longer than 1.2 meters. Also investigated is parametric excitation of the fundamental radial mode of a cylindrical cavity by modulating the height and thus the temperature. In this case, no driver was found to be capable of exceeding the threshold, regardless of the gas. Use of an electromagnetic wave source to modulate the temperature was also considered as a means of parametrically exciting the fundamental radial mode. Preliminary investigations show that sufficient heat conduction cannot occur over an acoustic cycle, indicating that this method is infeasible.

THIS PAGE INTENTIONALLY LEFT BLANK

TABLE OF CONTENTS

LIST OF FIGURES

LIST OF TABLES

THIS PAGE INTENTIONALLY LEFT BLANK

LIST OF SYMBOLS

A	amplitude, area
a	radius of cylindrical cavity or straight pipe
C	capacitance
c	sound speed
c_p	specific heat at constant pressure
E	energy
$\mathcal{E}$	energy density
$\dot{e}$	rate of energy dissipation per unit surface area
f	frequency
g	acceleration due to gravity, heat source function
h	height of cylindrical cavity
k	wavenumber, Boltzmann constant
ke	kinetic energy
J_n	Bessel's function of n^{th} order
j_{0n}	first extrema value of Bessel's function of n^{th} order
L	length of straight pipe or pendulum, inductance
p	pressure
pe	potential energy
Pr	Prandtl number
Q	quality factor
q	heat flux
R	resistance
r	radius
T	temperature
T_0	initial temperature
$\overline{T}$	time-averaged component of the temperature
T'	oscillatory component of the temperature
t	time
u	particle velocity
v	velocity
W	work
x	particle displacement
α	absorption coefficient
γ	ratio of heat capacities
δ_v	viscous penetration depth
δ_κ	thermal penetration depth
σ	thermal diffusivity
κ	thermal conductivity
η	dimensionless parametric drive amplitude

θ	angle measured from vertical
λ	wavelength
μ	coefficient of shear viscosity
ξ	displacement
ψ	temperature source function
$\overline{\psi}$	time-averaged component of the temperature source function
ψ'	oscillatory component of the temperature source function
ρ	density
ρ_0	equilibrium density
φ	velocity potential
ω	angular frequency

ACKNOWLEDGMENTS

I would like to thank my wife, Sherri, for all of her love and support. She has been a constant source of joy and happiness in my life. You have supported me through numerous patrols at sea, hectic refits in port, long hours at training commands, and through the long hours devoted to this thesis. You have made a tremendous difference in my life.

I would also like to thank my children, Kristen and Alex. Both of you continue to endure the many separations and long hours devoted to work. I love you and am proud of you both. I hope that I can instill in you both a sense of wonder and appreciation for learning.

Finally, I would like to thank my thesis advisor, Bruce Denardo. It has been a pleasure to work with and learn from you. Your enthusiasm about physics has been an inspiration to me. You have been one of those rare instructors who has made learning a pleasure. I am deeply indebted to you for the countless hours you have devoted to this thesis research and to furthering my understanding of parametric excitation.

THIS PAGE INTENTIONALLY LEFT BLANK

I. INTRODUCTION

Parametric excitation is the excitation of a resonant mode of a system by modulation of the value of a parameter upon which the frequency of the mode is dependent. This phenomenon can be more succinctly described as the excitation of a system at half the frequency with which a parameter is modulated. In order for parametric excitation to occur, the parameter must be modulated with an amplitude that is greater than a threshold value determined by the dissipation in the system. The mode then grows exponentially until limited by a nonlinearity of the system. Although the steady state response of a mode to parametric excitation is a nonlinear process, the onset of parametric excitation can be described using a linear system.

Perhaps the first recorded observation of parametric excitation was by the British physicist Michael Faraday (1831). A cylindrical container of water, which was caused to oscillate vertically, was found to have waves produced on the surface. Faraday observed that these surface waves had a frequency equal to one half the vertical oscillation frequency. Faraday's experiments were later duplicated and given a mathematical treatment by Lord Rayleigh (1883), who wrote, "Faraday arrived experimentally at the conclusion that there were two complete vibrations of the support for each complete vibration of the fluid." Another observation of parametric excitation was made by Melde (1859), who attached one end of a string to a prong of a tuning fork and the other end to a rigid structure. The string was attached to the tuning fork such that the tuning fork vibrated in a direction parallel to the length of the string, so that the tension was modulated. Melde was able to obtain transverse vibrations at frequency f when the tuning

fork was vibrated at frequency *2f*. In 1887, Rayleigh utilized the work of Hill (1886) to provide an analysis of Melde's work and a second mathematical explanation of Faraday's vertically oscillating cylinder.

An electromechanical example of parametric excitation was given by Lord Rayleigh (1945) in 1894. In *The Theory of Sound*, Rayleigh describes a "...pendulum, formed of a bar of soft iron and vibrating upon knife edges. Underneath is placed symmetrically a vertical bar electro-magnet, through which is caused to pass an electric current rendered intermittent by an interrupter whose frequency is twice that of the pendulum." Parametric excitation can also be observed in the electromagnetic equivalent of the spring oscillator. An oscillating current can be generated in a series LRC circuit containing an inductor L, capacitance C, and resistance R by periodically varying the capacitance or inductance. The capacitance can be varied by varying the distance between the plates of a parallel plate capacitor. Likewise, the inductance can be varied by periodically moving a core in and out of a coil. Mandelstam *et al.* (1935) varied the inductance by spinning a metal chopper wheel between the coils. Wright and Swift (1990) modulated the inductance by vibrating the bottom piece of a two-piece iron-core conductor. This vibration in turn modulated the air gap between the upper and lower pieces and hence the inductance. Utilizing this technique, large current amplitudes were produced.

The physical principle of parametric excitation in electrical and mechanical systems is fairly well understood. Parametric excitation is based on an external force pumping energy into a system. If the work done on the system during one half of the cycle is greater than the energy lost due to dissipation, then the mode will continue to

grow until it is limited by nonlinear effects. An advantage of parametrically exciting an acoustic mode is the possibility of achieving large response amplitudes that may be useful in thermoacoustic refrigerators, acoustic compressors, and acoustic pumps. The standard method of generating large acoustic amplitudes is by direct excitation with electromagnetic dynamic transducers. The typical means of increasing the amplitude of a sound wave is to increase the displacement of the electromagnetic driver. However, the driver is ultimately limited by one of two major limitations: *thermal limit* or *displacement limit*. The displacement limit occurs because of distortion or from the diaphragm parts being damaged by collision with the magnet or frame, or from exceeding the elastic limit of the suspension. The thermal limit is based on the material or the heat transfer capability of the voice coil of the driver. For a parametric drive, the drive is simply increased beyond the threshold value. Once the threshold is reached, the amplitude of the acoustic mode is amplified and is only limited by the nonlinearities of the system.

The nonlinearity that saturates the growth may arise from the oscillator or from a nonideal driving mechanism. The nonlinearity from a nonideal driving mechanism can occur in physical systems where the large response amplitude of the oscillator reduces the drive amplitude. Parametric drives may offer a practical advantage over direct drives in these situations. For example, if we consider a fixed response amplitude of a system, energy conservation implies that the same power input is required of a parametric drive as compared to a direct drive. If the directly driven oscillations are limited by the maximum excursion of an electromechanical driver, parametrically driven oscillations may be limited by the maximum current, which can lead to a greater power input and thus greater response amplitude.

In this thesis, we examine the feasibility of achieving parametric threshold in acoustic resonators. Specifically, we examine cylindrical acoustic resonators in which the length or height is modulated. Use of a microwave source to modulate the temperature is also considered. Parametric excitation has been achieved in a one-dimensional ultrasonic resonator by modulation of the cavity length (Adler and Breazeale, 1970), although not with the aim of achieving large amplitudes. Geometric modulation of Helmholtz resonators was studied by Prather (1999), who showed that geometric modulation of the resonator leads to turbulence which raises the threshold of parametric excitation to levels beyond that which can be readily attained.

The parametrically excited pendulum is discussed in Chapter II to provide a mathematical and physical description of parametric excitation. Chapter II also outlines the basic theory of parametric excitation as applied to a straight pipe and cylindrical cavity. The straight pipe refers to a cylinder in which the length is modulated in order to parametrically excite the fundamental *longitudinal* mode. The cylindrical cavity refers to a cylinder in which the height is modulated in order to parametrically excite the fundamental *radial* mode. Chapter III provides an analysis of modulating the length of a straight pipe while Chapter IV examines modulating the temperature of a cylindrical cavity by compressing the enclosed gas. In Chapter V, we consider the possibility of modulating the temperature of a gas by absorption of electromagnetic waves (for example, from a magnetron). Chapter VI discusses the conclusions and recommendations for future work.

II. BASIC PARAMETRIC EXCITATION THEORY

A. PARAMETRICALLY DRIVEN PENDULUM

The standard system for a theoretical discussion of parametric excitation is the pendulum whose length is periodically varied as shown in Fig. 2.1. If the net work done by the external force modulating the pendulum's length is greater than zero, then the amplitude of the pendulum increases. How energy is pumped into the system can be understood by calculating the work done by the external force over one oscillation of the pendulum. Following Chow (1995), the pendulum's length L is allowed to increase by a small amount ΔL when the pendulum is at its extreme position and the length is allowed to decrease by the same amount when the pendulum is in its vertical position. The work done by the external force when the pendulum is at its extreme position is

$$W = -mg(\cos\theta_0)\Delta L \qquad (2.1)$$

where m is the pendulum mass, g is the acceleration due to gravity and θ_0 is the pendulum's angle amplitude with respect to vertical. When the pendulum is vertical, the external force works against the weight of the mass and against the centrifugal force. Thus, the work done when the pendulum is vertical is

$$W = mg\Delta L + m\Delta L v_0^2 / L_0, \qquad (2.2)$$

where v_0 is the pendulum's velocity at the vertical position and L_0 is the ambient length of the pendulum. Combining Equations (2.1) and (2.2), the net work done by the external force over one cycle can be expressed as

$$W = 2\left[mg\Delta L(1-\cos\theta_0) + m\Delta L v_0^2 / L \right]. \tag{2.3}$$

If we assume that θ is small, then $\cos\theta_0 = 1-\frac{1}{2}\theta_0^{\,2}$, and $v_0 = \omega_0 L_0 \sin\theta_0 = \omega_0 L_0 \theta_0$, where $\omega_0 = \sqrt{g/L_0}$ is the pendulum's frequency of oscillation. With these approximations Eq. (2.3) becomes

$$W = 6\frac{\Delta L}{L_0}\frac{mv_0^2}{2}. \tag{2.4}$$

Thus, we see that the net work done by the pendulum is positive and is proportional to the energy of the pendulum. The rate at which energy is pumped into the system can be written as $dE/dt = 2\alpha E$ where α is an amplification constant. This differential equation is valid for weak drives where the rate of energy change per cycle is small. If α is sufficiently large such that the work done on the system is larger than the energy dissipated by the system, then the amplitude of the response will grow exponentially with time: Nonlinear effects will act to limit the amplitude of the response and the pendulum will achieve a steady state amplitude.

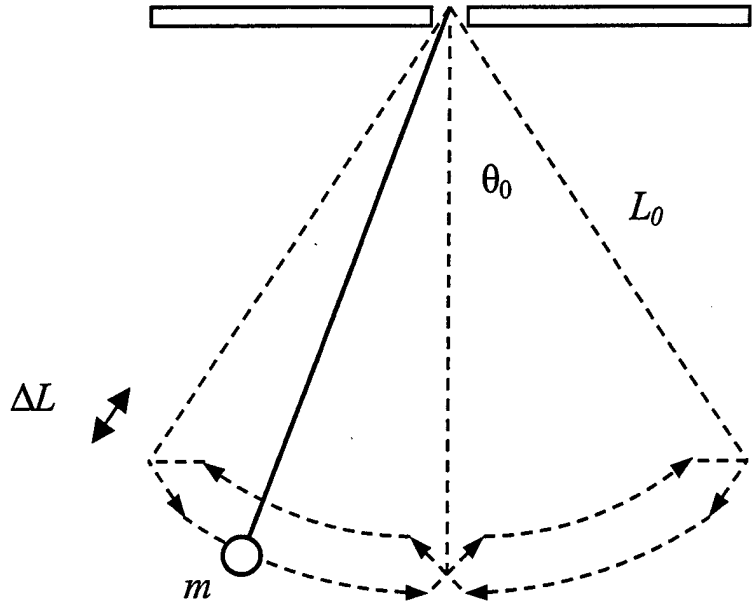

Figure 2.1. A parametric pendulum with periodically varying length.

The equation of motion for a parametrically excited system can be placed in a form known as the *Mathieu equation*, which can be written as

$$\ddot{x}(t)+\omega_0^2\left(1+\eta\cos\omega_D t\right)x(t)=0\,, \tag{2.5}$$

where x is the displacement, $\ddot{x}$ is the acceleration, t is the time, ω_0 is the natural linear frequency, ω_D is the drive frequency, and η is the dimensionless drive amplitude. Equation (2.5) is a linear differential equation that neglects the effects of dissipation. Note that Eq. (2.5) reduces to the equation for the simple harmonic oscillator for vanishing η.

Following Pinto (1993), the pendulum with periodically varying length can be placed in the form of the Mathieu equation. If we assume a polar coordinate system in which r is the radial coordinate and θ is the azimuthal coordinate, then $r(t)=L(t)$. The

pendulum length can be expressed as $L(t) = L_0 + \Delta L \cos \omega_D t$. Newton's second law in polar coordinates is

$$\vec{F} = m\left[\left(\ddot{r} - r\dot{\theta}^2\right)\hat{r} + \left(r\ddot{\theta} + 2\dot{r}\dot{\theta}\right)\hat{\theta}\right], \tag{2.6}$$

where $\vec{F}$ is the force, the dots denote differentiation with respect to time, and the carat denotes unit vectors. The angular component of Newton's second law in Eq. (2.6) becomes

$$-g \sin\theta = r\ddot{\theta} + 2\dot{r}\dot{\theta}, \tag{2.7}$$

where $-g \sin\theta$ is the acceleration in the azimuthal direction. Substituting the first and second derivatives of r into Eq. (2.7) and rearranging yields

$$\left(L_0 + \Delta L \cos \omega_D t\right)\ddot{\theta} - 2\omega_D \Delta L \sin \omega_D t \dot{\theta} + g \sin\theta = 0. \tag{2.8}$$

For small oscillations, Eq. (2.8) becomes

$$\left(1 + \eta \cos \omega_D t\right)\ddot{\theta} - 2\eta(\omega_D)\sin \omega_D t \dot{\theta} + \frac{g}{L_0}\theta = 0, \tag{2.9}$$

where we have divided through by L_0 and replaced $\Delta L / L_0$ with the dimensionless parametric drive amplitude η. Pinto (1993) states that Eq. (2.9) can be cast into Mathieu's equation by making the substitution $\xi = \left(1 + \eta \cos \omega_D t\right)\theta$. Evaluating and retaining only first order terms, we have verified that Eq. (2.9) becomes

$$\ddot{\xi} + \omega_0^2\left(1 + \eta \cos \omega_D t\right)\xi = 0 \tag{2.10}$$

where ω_0^2 is equal to g / L_0, the natural frequency of the pendulum.

B. CHARACTERISTICS OF PARAMETRIC EXCITATION

Although the linear Mathieu equation (Eq. (2.5) cannot be solved in closed form, its solutions, called *Mathieu functions*, have been studied extensively. A detailed study of Mathieu functions is beyond the scope of this thesis. However, the behavior of these functions provides an understanding of the subtleties of parametric excitation. The following characteristics of parametric excitation have been studied in detail by Bogoliubov and Mitropolsky (1961).

The first characteristic is that parametric excitation can occur when the following condition for the drive frequency is met:

$$\omega_n = 2\omega_0 / n, \tag{2.11}$$

where ω_0 is the fundamental frequency of the excited mode and $n = 1, 2\ldots$ However, as n increases, less energy is delivered to the oscillator by the external force. In this thesis, only the principal parametric resonance is considered ($n = 1$) due to its lower threshold value.

A second characteristic is that parametric excitation not only occurs at frequencies given by Eq. (2.11) but also in a range of frequencies around ω_n. This behavior is depicted in Fig. 2.2. As the dimensionless parametric drive amplitude is increased, this frequency band becomes larger. The region in which parametric excitation occurs is the *instability region.* As the order of the parametric resonance increases, parametric excitation occurs over a smaller frequency band for a given drive value.

Figure 2.2 shows the behavior for a dissipative and non-dissipative system. The effect of dissipation is to raise the threshold value. For the principal parametric resonance, the threshold value has been shown to equal $2/Q$, where Q is the quality factor of the excited mode. Thus, we see that a system with a small quality factor (large dissipative losses) will have a higher parametric threshold value. It can also be seen that for a given quality factor, the parametric threshold value increases as the order of the parametric resonance n increases.

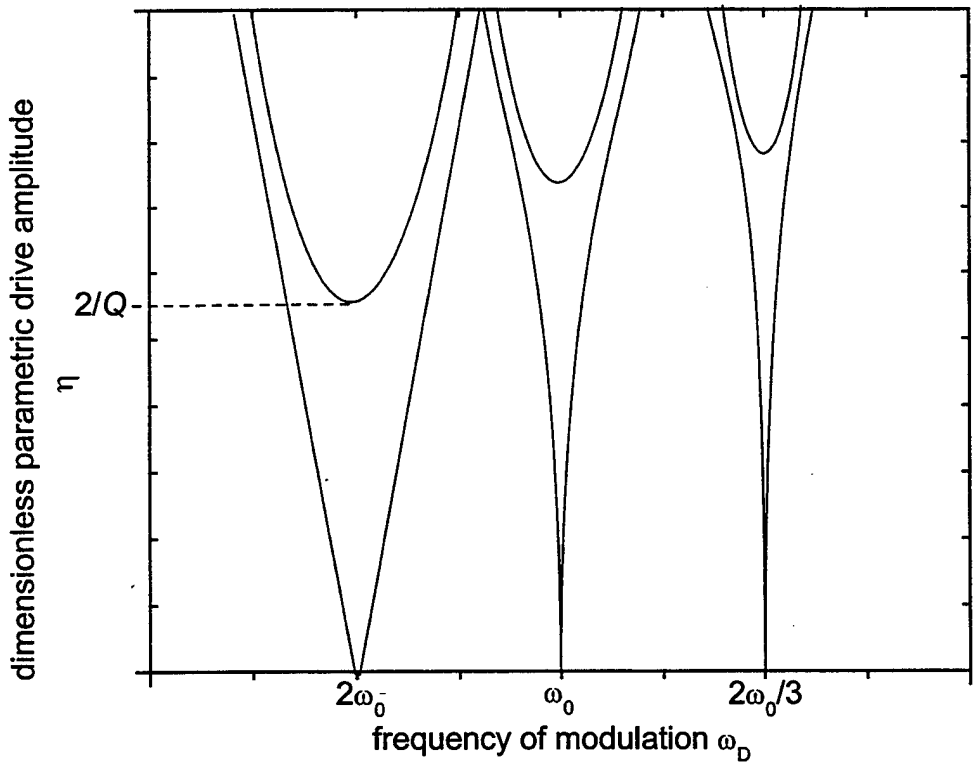

Figure 2.2. Sketch showing the regions of parametric excitation in a dissipative and non-dissipative system.

C. THEORY OF LENGTH MODULATION

We consider a closed pipe of length L_0. If the pipe is uniform, the natural frequencies of the modes are $\omega_n = n\pi c / L_0$, where n = 1, 2, 3... Because the frequency depends upon the length, it would appear possible to parametrically excite a mode if the length is appropriately modulated. We thus consider the length

$$L(t) = L_o + \Delta L \cos(2\omega t), \tag{2.12}$$

where ΔL is the peak drive displacement amplitude and 2ω is the drive frequency. For definiteness, we consider the fundamental (n =1) mode of the pipe. So that the drive does not directly excite the second mode, we imagine that the pipe has been detuned. This can be accomplished, for example, by a small constriction or enlargement at the center. This will respectively decrease or increase the natural frequency of the fundamental mode but will leave the frequency of the second mode approximately the same (Denardo and Alkov, 1994; Denardo and Bernard, 1996).

For a weak drive ($\Delta L \ll L_0$), the frequency of the mode is modulated according to $\omega_0\left[1-(\Delta L / L_0)\cos 2\omega t\right]$, where ω_0 is the natural frequency of the fundamental mode (which is $\omega_1 = \pi c / L_0$ for no detuning). For the ends of the pipe at x = 0 and approximately $x = L_o$, the displacement of the gas in the pipe is approximately of the form $\xi = f(t)\sin(\pi x / L_0)$ for a weak drive. Due to the frequency modulation, the equation of motion for the amplitude *f(t)* is expected to be the Mathieu equation

$$\frac{d^2 f}{dt^2} + \omega_o^2\left[1-\eta\cos(2\omega t)\right] f = 0, \tag{2.13}$$

where the dimensionless drive amplitude is $\eta = 2\Delta L / L_0$. In the presence of dissipation, the condition for parametric excitation is $\eta \geq 2/Q$ when $\omega = \omega_0$, where Q is the quality factor of the mode. Hence, the condition for parametric excitation of the fundamental mode of a straight resonator by length modulation is

$$\Delta L / L_o \geq 1/Q . \tag{2.14}$$

That is, the drive threshold for $\omega = \omega_0$ is $\Delta L / L_0 = 1/Q$.

A proper derivation of the Mathieu equation (Eq. (2.13)) would begin with the wave equation for the gas in the pipe. As we now show, Adler and Breazeale (1970) offer such a derivation, although they make several mistakes. The natural way to attempt to solve the problem is to impose the moving boundary condition on a general solution of the wave equation. However, this can be readily shown to only lead to the well-known solution corresponding to direct excitation.

The displacement $\xi(x,t)$ of the gas in the pipe satisfies the wave equation

$$\frac{\partial^2 \xi}{\partial t^2} - c^2 \frac{\partial^2 \xi}{\partial x^2} = 0 . \tag{2.15}$$

The ends of the pipe are taken to be at $x = 0$ and $x = L(t)$. Adler and Breazeale posit the following form of the displacement:

$$\xi(x,t) = f(t) \sin\left[\frac{\pi x}{L(t)}\right], \tag{2.16}$$

where we have specialized to the fundamental mode ($n = 1$ in the argument $n\pi x / L(t)$ of the sine). For convenience, we hereafter designate $f(t)$ by f and $L(t)$ by L. Equation

(2.16) satisfies the boundary condition at $x = 0$, and Adler and Breazeale state that it also satisfies the boundary condition at $x = L$. That is, $\xi(0,t) = \xi(L,t) = 0$. However, the latter boundary condition is $\xi(L,t) = L - L_0$ for the boundary displacement given in Eq. (2.12). More generally, the particle velocity at the end equals the velocity of the end of the pipe: $\partial\xi(L,t)/\partial t = dL/dt$. The displacement according to Eq. (2.16) can thus at most be justified for a weak drive.

Substitution of Eq. (2.16) into the wave equation (Eq. (2.15)) leads to

$$\left[\ddot{f} + \frac{c^2\pi^2}{L^2} f - \frac{\pi^2 x^2}{L^4}\dot{L}^2 f\right]\sin\left(\frac{\pi x}{L}\right) - \left[\ddot{L} f + 2\dot{L}\dot{f} - \frac{2}{L^2}\dot{L}^2 f\right]\frac{\pi x}{L^2}\cos\left(\frac{\pi x}{L}\right) = 0, \qquad (2.17)$$

where the dots denote time differentiation. The $\dot{L}^2 f$ term in the coefficient of the cosine term is absent in Adler and Breazeale's treatment, but this has no consequence due to their eventual approximation of a weak drive. Adler and Breazeale state that the coefficients of the sine and cosine in Eq. (2.17) must each vanish due to the orthogonality of these functions. However, this is incorrect due to the presence of the spatial dependence. To proceed correctly, we must now assume that the drive is weak. Neglecting the quadratic terms in $\dot{L}$ in Eq. (2.17) results in

$$\left(\ddot{f} + \frac{c^2\pi^2}{L^2} f\right)\sin\left(\frac{\pi x}{L}\right) - \left(\ddot{L} f + 2\dot{L}\dot{f}\right)\frac{\pi x}{L}\cos\left(\frac{\pi x}{L}\right) = 0. \qquad (2.18)$$

The spatial dependence is still present in the cosine term. However, if we multiply Eq. (2.18) by $\cos(\pi x/L)$, integrate from $x = 0$ to $x = L$, and use the orthogonality of the sine and cosine, we conclude that the coefficient of the cosine term must vanish:

$$\ddot{L}f + 2\dot{L}\dot{f} = 0. \tag{2.19}$$

It then follows from Eq. (2.18) that the coefficient of the sine term must vanish:

$$\ddot{f} + \frac{c^2\pi^2}{L^2} f = 0. \tag{2.20}$$

Substituting Eq. (2.12) for L and retaining only linear terms in ΔL due to the assumption of weak drive, yields the Mathieu equation (Eq. (2.13)), where $\omega_0 = \pi c / L_0$ and $\eta = 2\Delta L / L_0$.

Equation (2.19) must also be satisfied. Adler and Breazeale claim that the equation has a solution that coincides with a solution of Mathieu's equation, which does not appear to be true. For $f = A\sin\omega t + B\cos\omega t + \{\text{smaller-amplitude higher harmonics}\}$ and L given by Eq. (2.12), Adler (1969) shows that Eq. (2.19) is satisfied for first-order terms which have frequency ω. Because the analysis is only valid to this order, Eq. (2.19) is then satisfied. This is readily confirmed to be true.

For a weak drive with ω approximately equal to ω_0, it must be true that f is approximately given by the expression in the previous paragraph. Furthermore, Eq. (2.18) is satisfied for all f in the absence of a drive ($\dot{L} = 0$ for all time). However, the equation can be separated and thus exactly solved:

$$f(t) = f(0)\sqrt{\frac{\dot{L}(0)}{\dot{L}(t)}}, \tag{2.21}$$

which shows that f *diverges* at points in time when $\dot{L} = 0$. For the standard length modulation (Eq. (2.12)), this occurs twice each cycle of the drive and thus four times

each cycle of the response. Furthermore, this occurs regardless of the smallness of the drive amplitude, as long as it is not zero. Such a solution clearly contradicts the correct behavior of the system.

The only way to resolve this contradiction is if the initial form of the solution (Eq. (2.16)) is invalid. We thus conclude that Adler and Breazeale's derivation of Mathieu's equation for length modulation of a straight acoustic resonator is incorrect. To our knowledge, a proper derivation does not yet exist. Moreover, there does not yet exist a physical derivation showing directly (without Mathieu's equation) that the drive can transfer a net amount of energy over one cycle to the response, thus leading to parametric excitation. The correctness of Mathieu's equation may thus be questioned here. However, although their derivation is incorrect, Adler and Breazeale present unquestionable experimental evidence for the parametric excitation of an acoustic resonator by length modulation. In fact, they employ the theoretical drive amplitude threshold to accurately determine absorption constants experimentally for various liquids. We thus conclude that the Mathieu equation given by Eq. (2.13) describes parametric excitation by length modulation of an acoustic resonator, but that a proper derivation of this equation does not yet exist.

D. THEORY OF TEMPERATURE MODULATION

We consider a closed pipe whose ends are at $x = 0$ and $x = L$, where an external source *uniformly* modulates the temperature of the gas in the pipe. The frequency of an acoustic mode in the pipe depends upon the speed of sound, which depends upon the

temperature. It should thus be possible to parametrically excite a mode by appropriate modulation of the temperature. We show below that Mathieu's equation can indeed be derived in this case, which shows that parametric excitation should be possible. However, we also give a physical argument that suggests that parametric excitation may *not* be possible in this case. We have not yet resolved this conflict.

The temperature modulation can be accomplished, for example, by varying the radius of the pipe if the walls are adiabatic and the wavelength corresponding to the drive frequency is large compared to the radius. A similar situation is examined in detail in Ch. IV for the case of a cylindrical cavity whose height is modulated. Another possibility is to subject the gas to electromagnetic radiation whose intensity is modulated. This is examined in Ch. V.

To derive the linear wave equation for one-dimensional motion of the gas in the presence of a time-varying speed of sound, consider an element of gas of thickness dx. The mass of the element is $\rho_0 A dx$ to first order, where ρ_0 is the ambient density and A is the cross-sectional area of the pipe. The acceleration is $\partial v/\partial t$, where v is the particle velocity. The net force is due to the difference in pressure on the ends of the element, and is thus $-A(\partial p/\partial x)dx$. Newton's second law then yields $-\partial p/\partial x = \rho_0 \partial v/\partial t$. The rate of change of the mass of an element is $A(\partial \rho/\partial t)dx$, where ρ is the density. This arises due to a difference in the mass flow rate at the ends of the element, and thus can also be expressed as $-A\rho_0(\partial v/\partial x)dx$. The equation of continuity is therefore $\partial \rho/\partial t = -\rho_0 \partial v/\partial x$. The ambient density ρ_0 in a closed pipe is not a function of temperature and thus not a function of time. We can then eliminate the velocity by

adding the x-derivative of the first equation to the t-derivative of the second equation, which results in $\partial^2\rho/\partial t^2 - \partial^2 p/\partial x^2 = 0$. Let p_0 be the ambient pressure at temperature T. The acoustic deviation of the pressure from p_0 is $p' = c^2\rho'$, where ρ' is the density deviation and c is the speed of sound at temperature T. Substituting $p = p_0 + p' = p_0 + c^2 p'$ and $\rho = \rho_0 + \rho'$ into the previous equation, and noting that p_0 and c are not functions of x, results in

$$\frac{\partial^2\rho'}{\partial t^2} - c^2\frac{\partial^2\rho'}{\partial x^2} = 0. \tag{2.22}$$

Hence, the density variation is described by the standard wave equation even when the speed of sound is a function of time (but not space). It can be shown that this equation does not occur for the pressure variation p'.

The square speed of sound is proportional to absolute temperature: $c^2 \propto T$. For the temperature modulation $T = T_0\left[1+\eta\cos(2\omega t)\right]$, where $\eta = \Delta T/T_0$, the wave equation (2.22) thus becomes

$$\frac{\partial^2\rho'}{\partial t^2} - c_0^2\left[1+\eta\cos(2\omega t)\right]\frac{\partial^2\rho'}{\partial x^2} = 0 \tag{2.23}$$

where c_0 is the speed of sound at temperature T_0. In the dimensionless drive amplitude η, it is important to note that T_0 is the *absolute* temperature.

To determine the effect of the temperature modulation on a mode of the pipe, we set $\rho' = f(t)\cos(n\pi x/L)$, where $n = 1, 2, 3, \ldots$ in Eq. (2.23). The result is

$$\frac{d^2 f}{dt^2} + \omega_n^2 \left[1 + \eta \cos(2\omega t)\right] f = 0 \qquad (2.24)$$

where the frequency of the n^{th} mode is $\omega_n = n\pi c / L$. Equation (2.24) is a standard form of Mathieu's equation, so we conclude that it is theoretically possible to parametrically excite an acoustic mode by temperature modulation. The greatest rate of growth of the amplitude of a mode occurs when $\omega = \omega_n$ and when the phase of the mode is such that the turning points occur at the positive-slope zero crossings of the drive. That is, there is a 45° phase shift between the response and the drive.

To attempt to gain a physical understanding of this parametric excitation, we consider the fundamental mode in the pipe (Fig. 2.3). It is conceptually convenient to consider a temperature modulation where the change in temperature is "lumped" in time. Specifically, the temperature is abruptly increased at a turning point of the standing wave and abruptly decreased at equilibrium (Fig. 2.4). This phase corresponds to the theoretical maximum growth rate of the response. Our arguments can be extended to the more-common drives, which vary sinusoidally in time.

The acoustical potential energy density is $pe = c^2 \rho^2 / 2\rho_0$ and the kinetic energy density is $ke = \rho_0 v^2 / 2$. The temperature modulation alters the speed of sound but not the density or the particle velocity directly. The modulation thus increases the energy of the standing wave at the turning points but does not alter the energy at equilibrium, so the energy of the standing wave will grow.

The situation is analogous to a mass on a spring, where the spring constant is abruptly increased at turning points of the motion and abruptly decreased at equilibrium.

The mass thus has a greater acceleration while it is moving toward equilibrium, and less deceleration as it is moving away, so its amplitude grows. This is consistent with energy conservation because work is required to stiffen the spring at a turning point of the motion, but no work is required to weaken the spring at equilibrium. In all cases where parametric excitation occurs, the drive must add more energy than it removes.

This is a problem with the acoustics argument, however, because it appears that the same amount of heat is added and removed. If parametric excitation is possible for this system, the standing wave must somehow cause the source to add more heat than is removes. The resolution of this conflict is important for several reasons. First, it may be that parametric excitation by temperature modulation is impossible. That is, the above physical argument and the derivation of Mathieu's equation may be incorrect. Second, if parametric excitation by temperature modulation is possible, a physical understanding is important because actual drives may differ from the idealized temperature modulation drive. In an experiment, it would be important to understand possible effects of such nonideal drives.

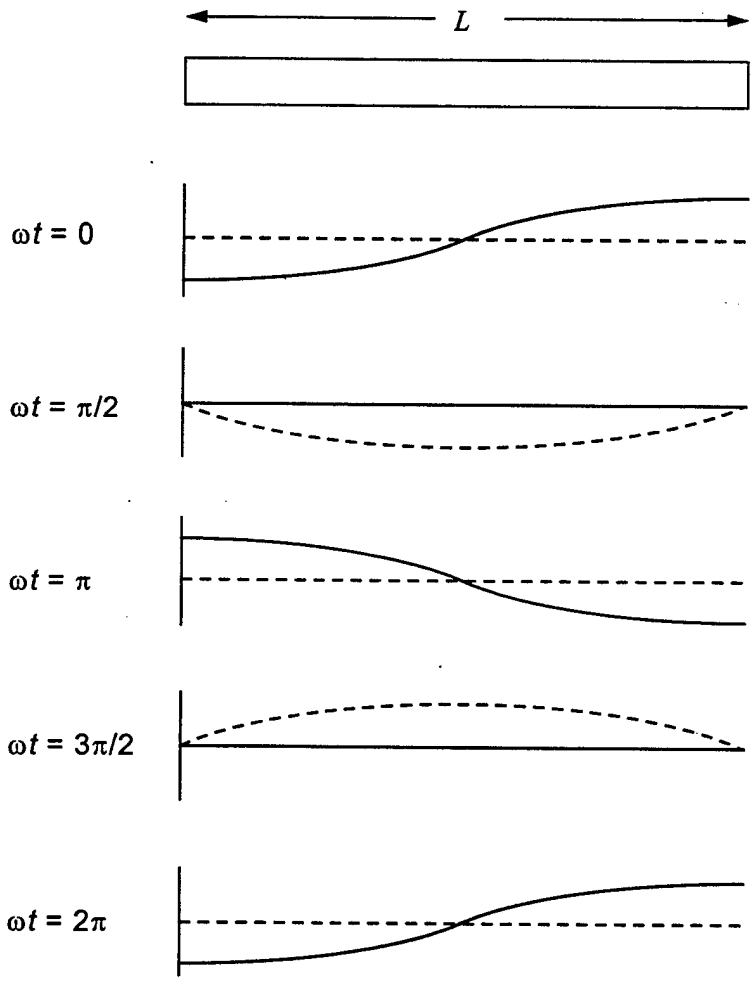

Figure 2.3. Density deviation ρ'(solid curves) and particle velocity v (dashed curves) corresponding to the fundamental acoustic mode of a closed pipe.

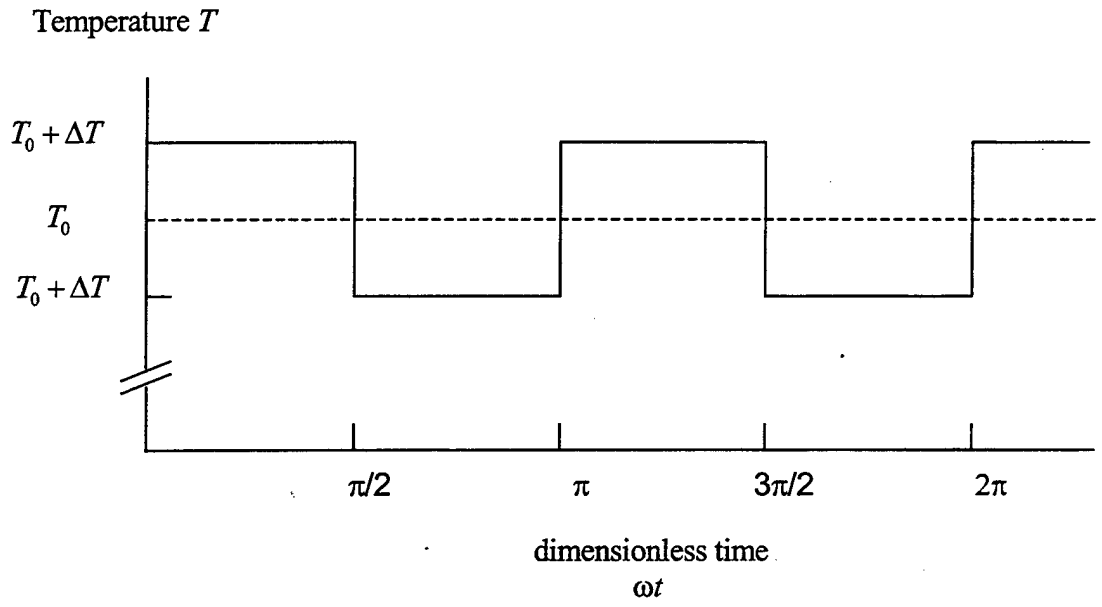

Figure 2.4. Temperature modulation of the gas in a closed pipe, as a function of time. The temperature is spatially uniform, and "lumped" in time. The frequency is twice that of the fundamental acoustic mode (Fig. 2.3).

THIS PAGE INTENTIONALLY LEFT BLANK

III. LENGTH MODULATION OF A CLOSED PIPE

In this chapter, we consider length modulation of a straight pipe in order to parametrically excite an acoustic mode. Because the natural frequency of a longitudinal mode of a straight pipe depends upon its length, parametric excitation can occur in principle. We investigate the experimental feasibility of this for the fundamental longitudinal mode.

A. DESCRIPTION

We consider the excitation of the fundamental longitudinal mode of a cylindrical resonator of length L and radius a. Figure 3.1 provides a representation for the case to be considered. The parameter to be varied for this case is the cylinder length L. Since the longitudinal modes are defined by the cylinder length, varying the length at twice the frequency of the fundamental longitudinal mode should result in the parametric excitation of that mode if the drive amplitude is sufficiently large. It is important to note that the resonant frequencies of the longitudinal modes are harmonics of the fundamental longitudinal mode. Thus, parametrically exciting the fundamental mode by length modulation will also directly excite the second longitudinal mode. This unwanted effect could be eliminated by detuning the resonator to prevent the direct excitation of the second longitudinal mode (refer to Sec. II.C).

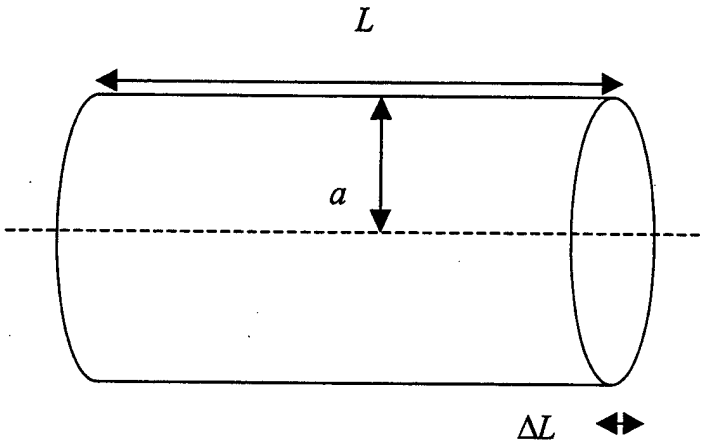

Figure 3.1. Length modulation of a closed pipe.

B. QUALITY FACTOR AND PARAMETRIC THRESHOLD

Assume a fluid in a pipe (as shown in Fig. 3.1) of cross sectional area S and ambient length L is driven by a piston at $x = 0$ and is rigidly terminated at $x = L$. The longitudinal (plane wave) resonances occur for $k_n L = n\pi$, where k_n is the wavenumber of the n^{th} mode, for $n = 1, 2...$ The wavenumber for the fundamental longitudinal mode is then given by $k_1 = \pi / L$. The fundamental longitudinal resonant frequency is given by

$$f_0 = c/2L, \tag{3.1}$$

where c is the speed of sound. The pressure and velocity profiles for the fundamental longitudinal mode are shown in Figure 3.2.

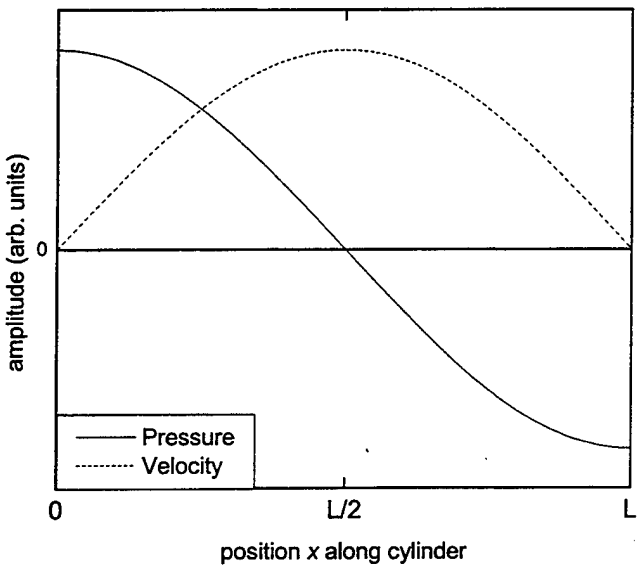

Figure 3.2. Profile of fundamental longitudinal mode of a cylindrical resonator.

The quality factor for this resonance is determined by the amount of thermal and viscous losses that occur in the cavity. Kinsler *et al.* (2000) derive the following expressions for the viscous and thermal absorption coefficients per unit length, where a is the pipe radius, μ is the coefficient of shear viscosity, γ is the ratio of specific heats, κ is the thermal conductivity, ρ_0 is the fluid density, ω is the angular frequency, and Pr is the Prandtl number:

$$\alpha_{\omega\eta} = (1/ac)\sqrt{\mu\omega/\rho_0}\,, \tag{3.2}$$

$$\alpha_{\omega\kappa} = \left(\frac{1}{ac}\right)\frac{(\gamma-1)}{\sqrt{\mathrm{Pr}}}\sqrt{\frac{\omega\mu}{2\rho_0}}\,. \tag{3.3}$$

It should be noted that the Prandtl number provides a measure of the relative effects of viscosity to thermal conduction. These expressions are valid for wide pipes; i.e., $a \gg \delta_\nu$, where δ_ν is the viscous penetration depth $\left(\delta_\nu = \sqrt{2\mu/\omega\rho}\right)$. The viscous penetration

depth δ_v is the distance required for the particle velocity amplitude to increase from zero at the wall to $1/e$ of its bulk value (Blackstock, 2000). The thermal penetration depth is the region near the wall where the flow changes from adiabatic to isothermal. The combined absorption coefficient is found by adding the viscous and thermal absorption coefficients and is thus given by

$$\alpha = \left(\frac{1}{ac}\right)\sqrt{\frac{\mu\omega}{2\rho_0}}\left(1+\frac{\gamma-1}{\sqrt{\mathrm{Pr}}}\right). \tag{3.4}$$

This expression is based on the assumption that the boundary layer is small compared to the cylinder radius but not so small that bulk thermoviscous losses are important. Quantitatively, Blackstock (2000) writes this assumption as

$$\delta_v << a << \frac{c_0^2}{\omega_0^2 \delta_v}. \tag{3.5}$$

Kinsler *et al.* (2000) state that the quality factor Q for a mode can be theoretically calculated from the following expression

$$Q = k/2\alpha. \tag{3.6}$$

Note that this does not include losses at the endcaps, which is normally small compared to losses along the cylindrical wall. Also, Eq. (3.7) does not include the possible lowering of the quality factor due to the presence of a driver at one (or both) ends of the pipe. Substituting Eq. (3.4) into Eq. (3.6) yields

$$Q = a\sqrt{\frac{\rho_0\omega}{2\mu}}\Bigg/\left(1+\frac{\gamma-1}{\sqrt{\mathrm{Pr}}}\right). \tag{3.7}$$

The dimensionless parametric drive threshold η_{th} is given by $\eta_{th} = 2/Q$. Using Eq. (3.7), the parametric drive threshold for the longitudinal modes in a closed pipe is

$$\eta_{th} = \frac{2}{a}\sqrt{\frac{2\mu}{\rho_0 \omega}}\left(1+\frac{\gamma-1}{\sqrt{\mathrm{Pr}}}\right). \tag{3.8}$$

If we consider the case of the fundamental longitudinal mode with $\omega = \pi c/L$, then Eq. (3.8) becomes

$$\eta_{th} = \frac{2}{a}\sqrt{\frac{2\mu L}{\pi \rho_0 c}}\left(1+\frac{\gamma-1}{\sqrt{\mathrm{Pr}}}\right). \tag{3.9}$$

Although Eq. (3.9) does not explicitly contain a frequency term, it is contained implicitly because it specifically applies to the fundamental longitudinal mode. The frequency of the fundamental longitudinal mode is dependent on the pipe geometry and the speed of sound in the enclosed gas. Equation (3.8) is applicable to the parametric excitation of any longitudinal mode in a closed pipe. We consider the fundamental longitudinal mode because it will require a lower drive frequency than higher modes.

The modulated parameter for the geometrical case is the length of the cylindrical resonator. The fundamental longitudinal mode's angular frequency ω is inversely proportional to the pipe length L. Using a first order approximation, we find that

$$\omega^2 = \omega_0^2\left(1-\frac{2\Delta L}{L}\cos 2\omega t\right). \tag{3.10}$$

Thus, the dimensionless parametric drive amplitude can be expressed as $\eta = 2\Delta L/L$. Substituting this expression into Eq. (3.9), we find that the required displacement amplitude to parametrically excite the fundamental longitudinal mode is given by

$$\Delta L = \frac{L^{3/2}}{a}\sqrt{\frac{2\mu}{\pi\rho_0 c}}\left(1+\frac{\gamma-1}{\sqrt{\mathrm{Pr}}}\right). \tag{3.11}$$

Note that this expression can be decomposed into a term dependent upon the geometry of the pipe and another term dependent on the gas contained in the pipe.

C. EFFECTS OF USING VARIOUS GASES IN THE CLOSED PIPE

We now consider the case of a cylindrical resonator filled with different gases in order to understand their effect on the parametric drive threshold. Appendix A lists various thermodynamic and fluid properties of air, helium, carbon dioxide and sulfur hexafluoride at 25 °C and 1 atm. Substituting the values from Appendix A into Eq. (3.11), the threshold parametric drive amplitude ΔL for the fundamental longitudinal mode in SI units becomes

He: $$\Delta L = 4.966\times10^{-4}\frac{L^{3/2}}{a}, \tag{3.12}$$

Air: $$\Delta L = 2.508\times10^{-4}\frac{L^{3/2}}{a}, \tag{3.13}$$

CO_2: $$\Delta L = 1.865\times10^{-4}\frac{L^{3/2}}{a}, \tag{3.14}$$

SF_6: $$\Delta L = 1.202\times10^{-4}\frac{L^{3/2}}{a}, \tag{3.15}$$

where a, L, and ΔL are expressed in meters. The results of Eqs. (3.12) to (3.15) are plotted in Figures 3.3, 3.4, 3.5 and 3.6 along with the required drive frequency for each closed pipe length. These equations show that using a heavier gas can significantly

reduce the parametric drive threshold. The use of sulfur hexafluoride over air will reduce the parametric drive threshold by slightly more than a factor of two. On the other hand, the use of helium would result in a parametric drive threshold of approximately twice the value for air. Figures 3.7, 3.8 and 3.9 illustrate the significant differences in the parametric drive threshold for the various gases.

It is worth mentioning the quality factor Q for a matter of comparison. For a straight pipe of radius 20 cm and length 1.0 m, Q is 800 for air, 1075 for CO_2, and 1660 for SF_6. Note that the quality factor is inversely proportional to the square root of the length. Thus, decreasing the length by half will result in the Q increasing by a factor of 1.4.

While sulfur hexafluoride has a lower threshold drive amplitude than the other gases, it has a much more significant effect on the frequency of the fundamental mode. If we consider a one meter long closed pipe at 25 °C, the fundamental frequency using sulfur hexafluoride is 136 Hz. For the same resonator containing air, the fundamental frequency is 346 Hz. If an electromagnetic driver is used to vary the length of the closed pipe, the maximum driver displacement is dependent on the frequency. For a driver operating in the mass controlled region, the driver displacement for a fixed current is inversely proportional to the square of the frequency. Thus, using sulfur hexafluoride lowers the parametric drive frequency by the ratio of the speed of sound or approximately a factor of 2.5. This lower drive frequency can increase the drive amplitude by a factor of 6.3 (assuming the drive operates in the mass controlled region). Figures 3.10, 3.11 and 3.12 show the threshold parametric drive amplitudes for a given closed pipe length and as a function of the closed pipe radius, for various gases. The theoretical values for

various electromechanical drivers are also plotted in Figures 3.10 through 3.12. The closed pipe radius for these drivers was chosen to match their active surface area.

Of the electromechanical drivers considered, the EVX-150A driver generated the largest displacement. Figure 3.13 shows the threshold drive amplitude and the EVX-150A displacement amplitude as functions of length of the resonator. The figure shows that the EVX-150A is always capable of exceeding the threshold amplitude for a sulfur hexafluoride filled straight pipe. For carbon dioxide, the EVX-150A is capable of exceeding the threshold when the length is greater than approximately 1.2 m. For air, the EVX-150A is not capable of exceeding the threshold amplitude. However, it is possible to increase the drive amplitude by attaching an EVX-150A driver at each end of the resonator.

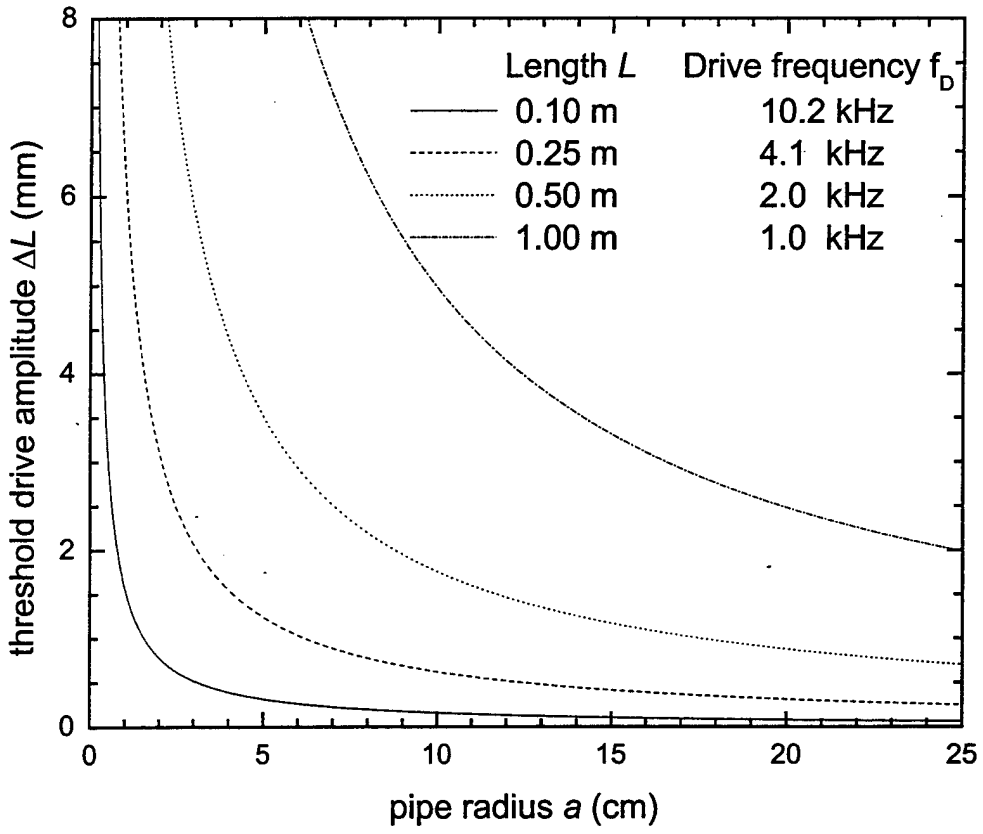

Figure 3.3. Threshold parametric drive amplitude for the fundamental longitudinal mode of a helium filled closed pipe at 25 °C and 1 atm.

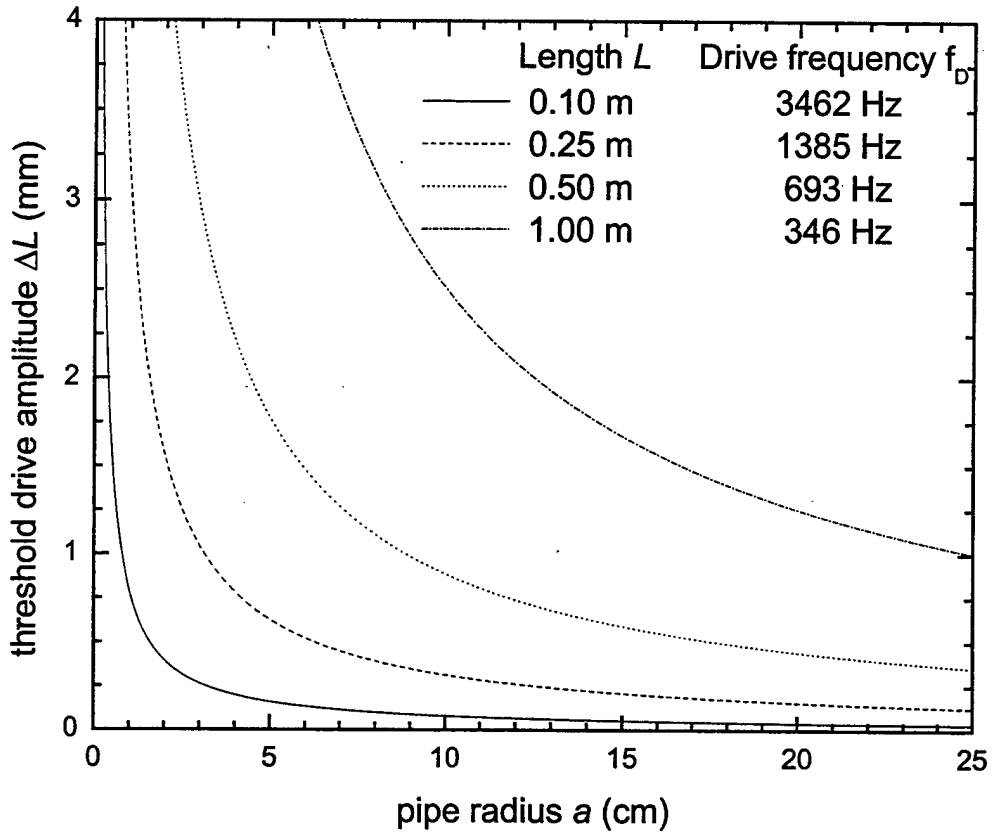

Figure 3.4. Threshold parametric drive amplitude for the fundamental longitudinal mode of an air filled closed pipe at 25 °C and 1 atm.

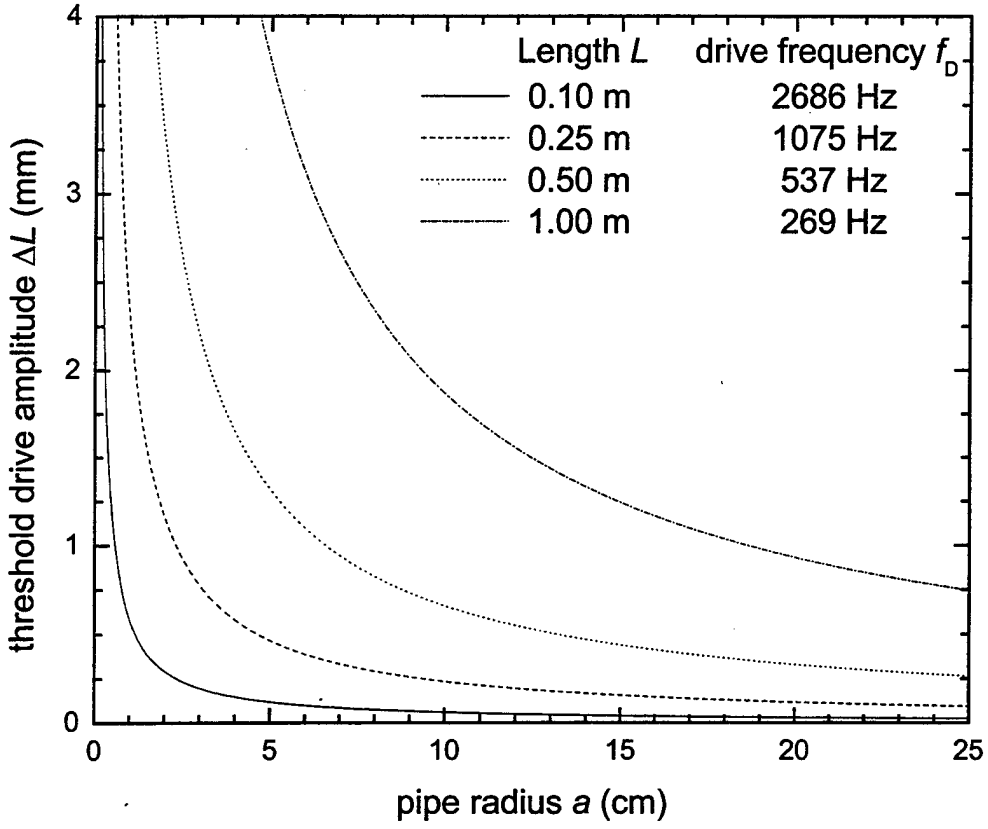

Figure 3.5. Threshold parametric drive amplitude for the fundamental longitudinal mode of a carbon dioxide filled closed pipe at 25 °C and 1 atm.

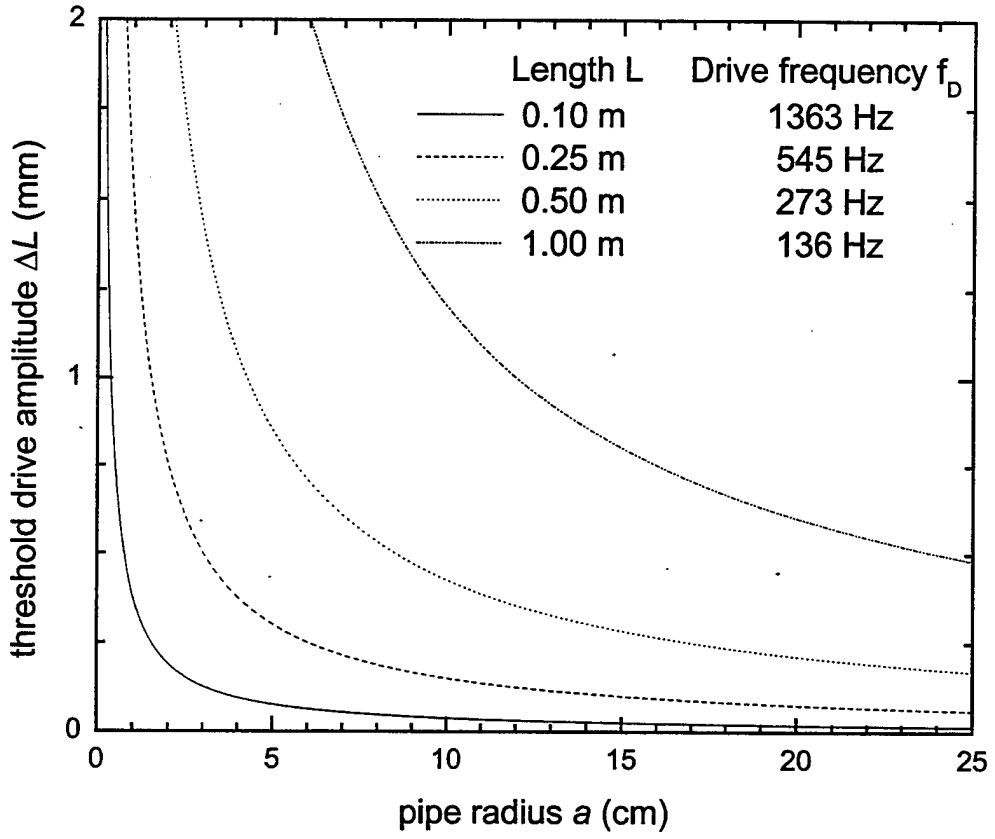

Figure 3.6. Threshold parametric drive amplitude for the fundamental longitudinal mode of a sulfur hexafluoride filled closed pipe at 25 °C and 1 atm.

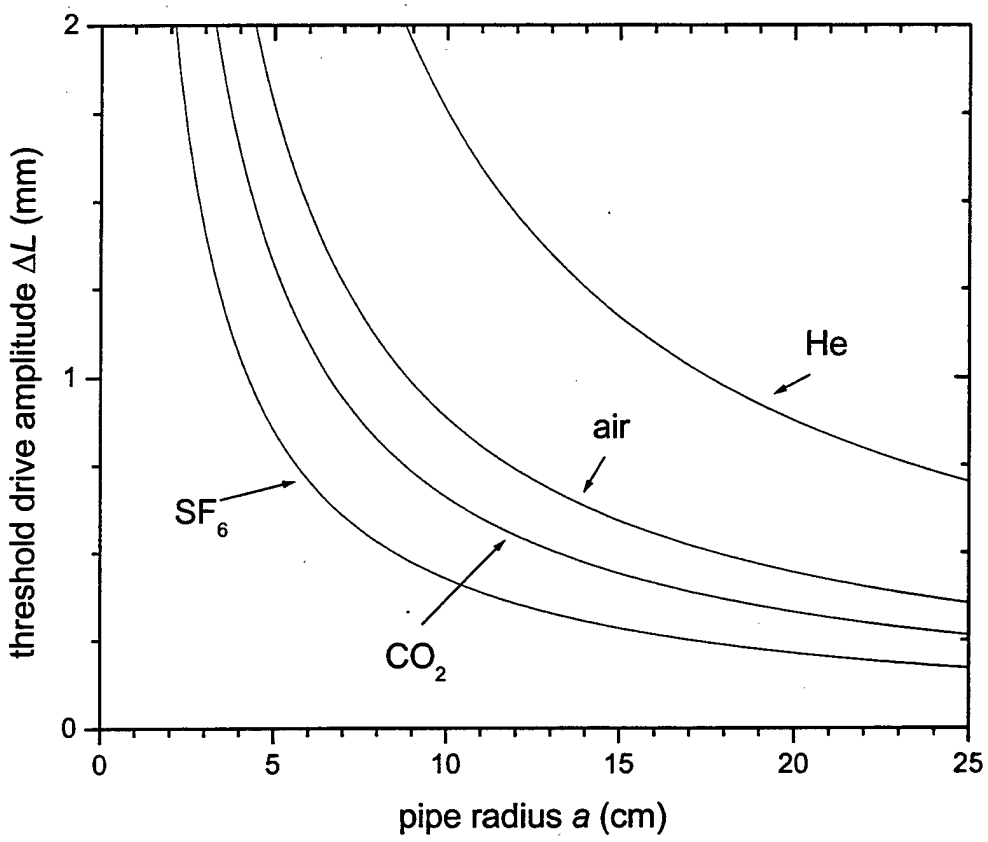

Figure 3.7. Threshold parametric drive amplitude for a 50 cm long closed pipe filled with various gases at 25 °C and 1 atm.

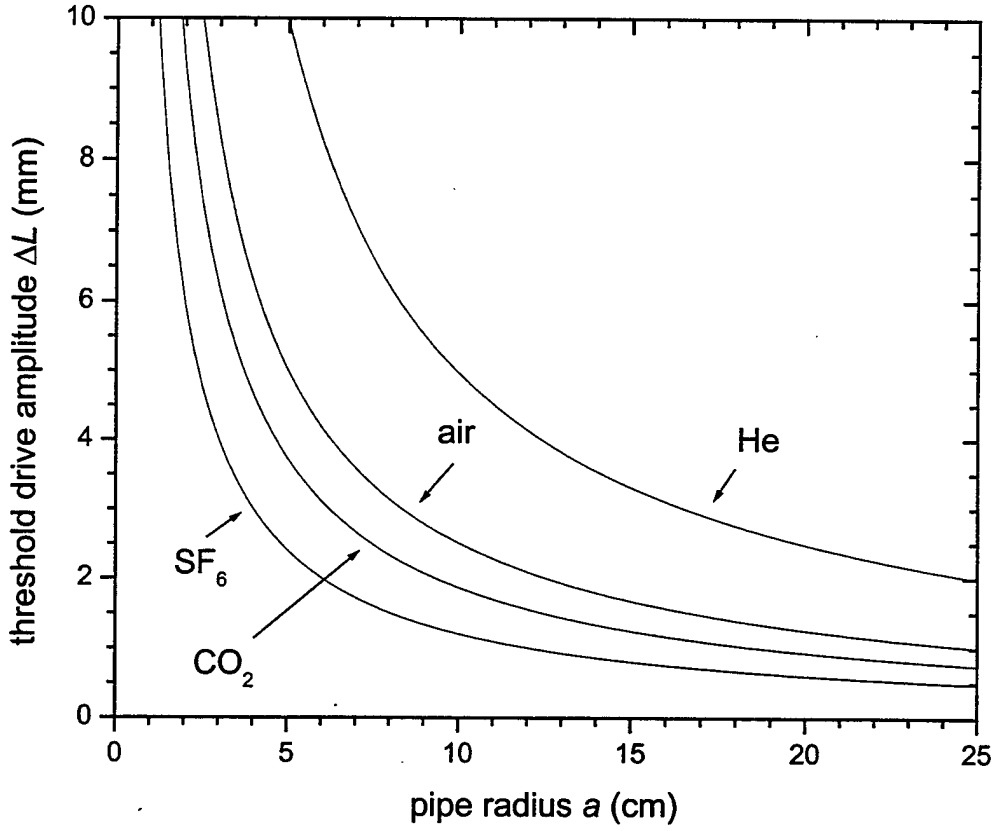

Figure 3.8. Threshold parametric drive amplitude for a 1 m long closed pipe filled with various gases at 25 °C and 1 atm.

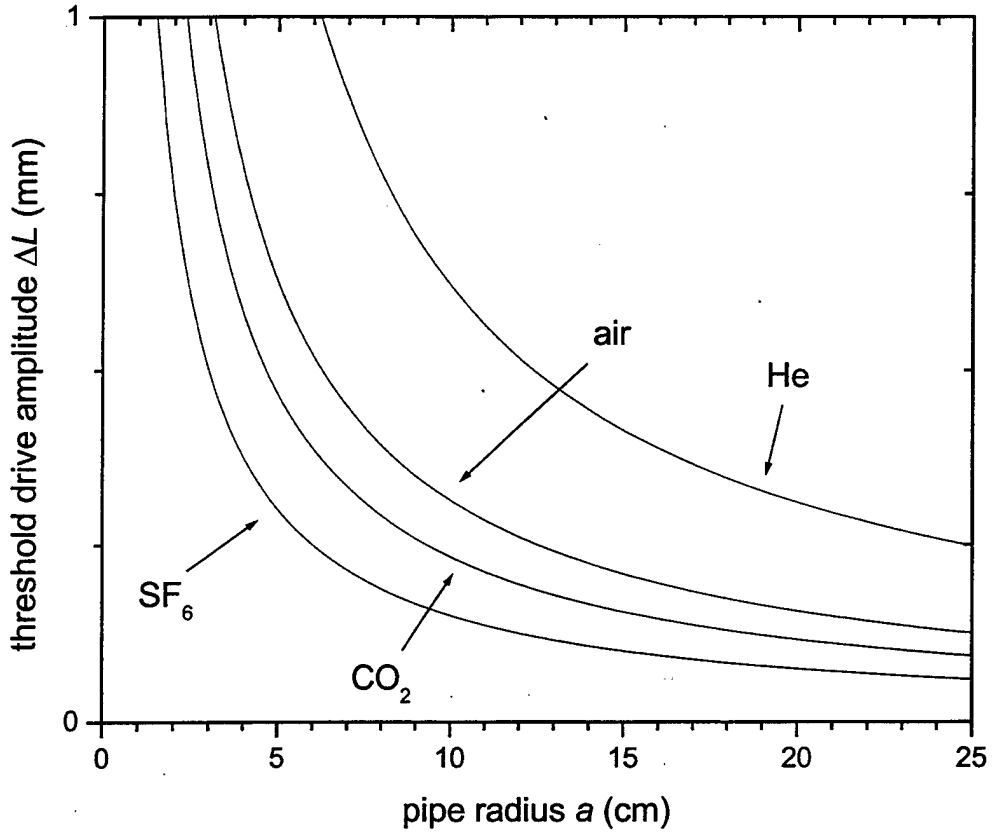

Figure 3.9. Threshold parametric drive amplitude for a 2 m long closed pipe filled with various gases at 25 °C and 1 atm.

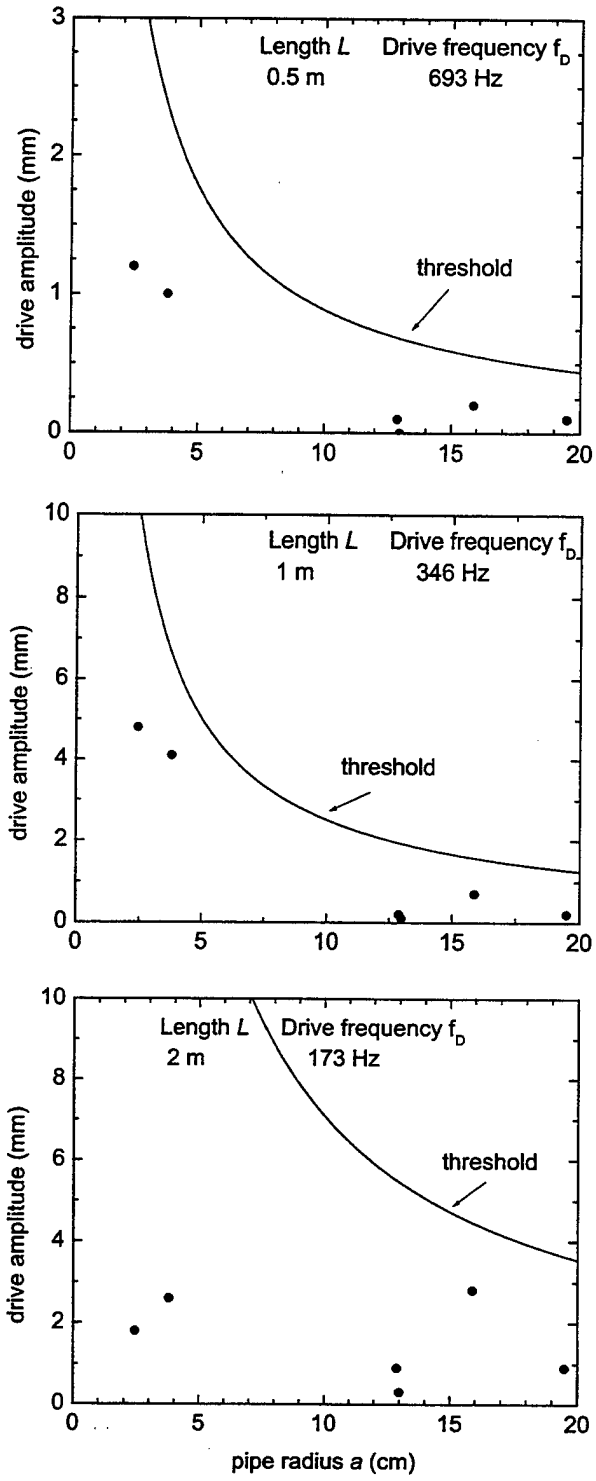

Figure 3.10. Threshold parametric drive amplitude (curve) and various driver amplitudes (points) for a closed pipe containing air at 25 °C and 1 atm.

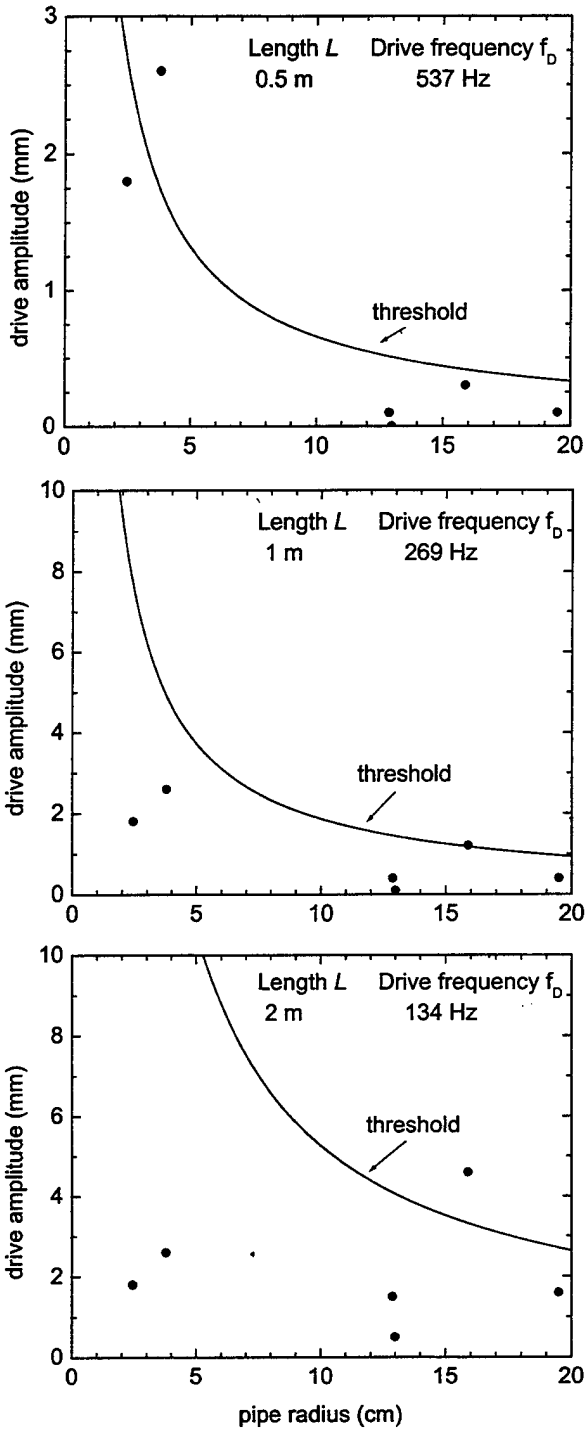

Figure 3.11. Threshold parametric drive amplitude (curve) and various driver amplitudes (points) for a closed pipe containing carbon dioxide at 25 °C and 1 atm.

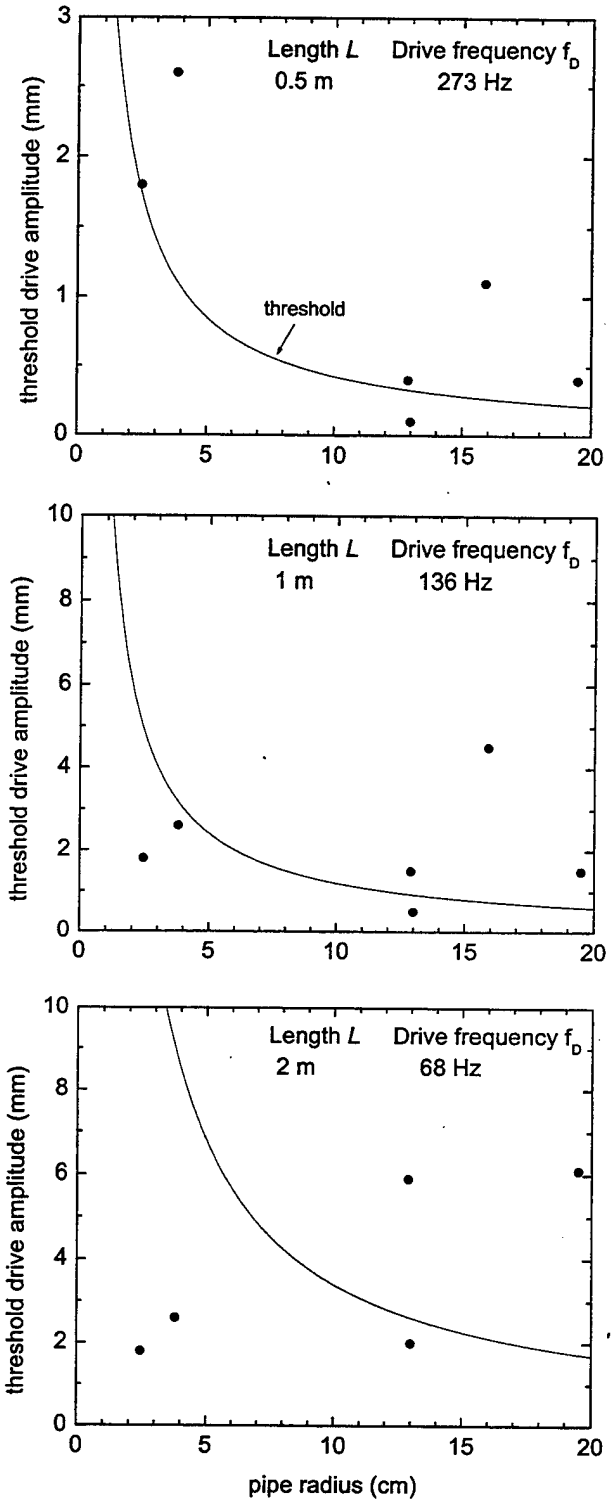

Figure 3.12. Threshold parametric drive amplitude (curve) and various driver amplitudes (points) for a closed pipe containing sulfur hexafluoride at 25 °C and 1 atm.

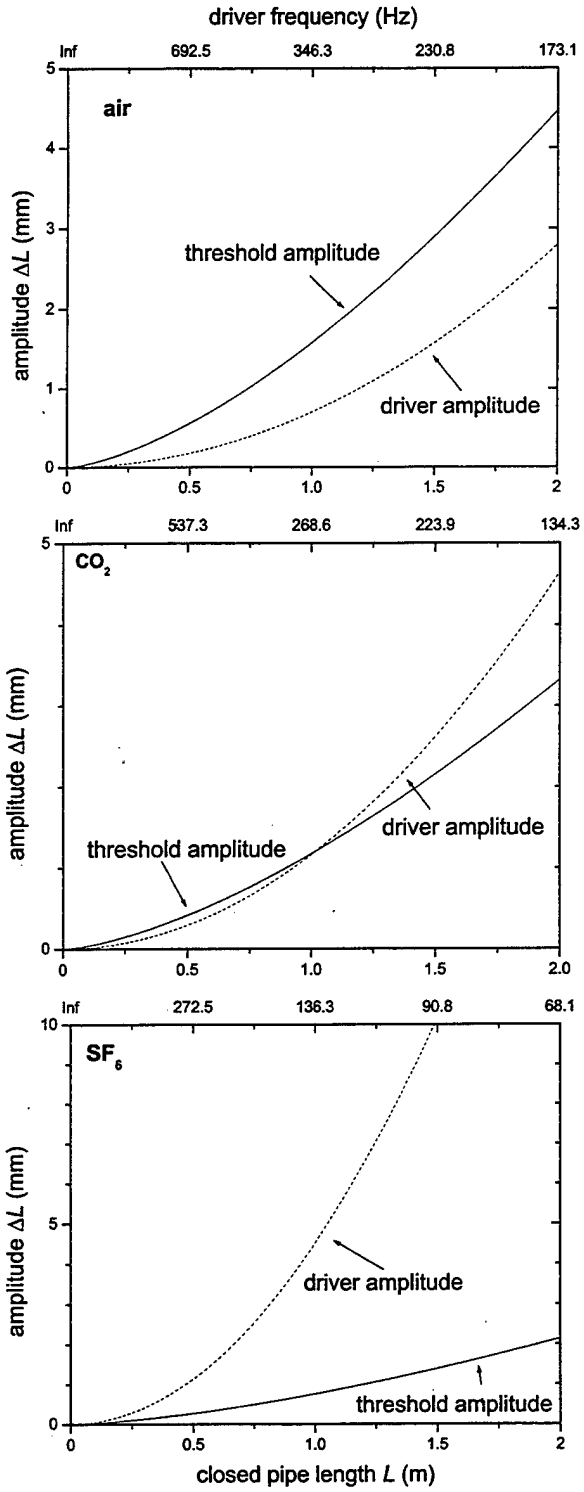

Figure 3.13. Threshold parametric drive amplitude and EVX-150A amplitude for a closed pipe containing various gases at 25 °C and 1 atm.

THIS PAGE INTENTIONALLY LEFT BLANK

IV. HEIGHT MODULATION OF A CYLINDRICAL CAVITY

In this chapter, we consider height modulation of a cylindrical cavity in order to parametrically excite an acoustic mode. Modulating the height modulates the temperature and thus the speed of sound. Because the natural frequency of a mode depends upon the speed of sound, parametric excitation can occur in principle. We investigate the experimental feasibility of this for the fundamental radial mode.

A. DESCRIPTION

We consider a cylinder of radius a and height h as shown in Fig. 4.1. In cylindrical coordinates (r, z, θ), the standing wave solution to the linear wave equation for the pressure can be written as

$$p_{lmn} = A_{lmn} J_m(k_{mn} r)\cos(m\theta + \psi_{lmn})\cos(k_l z)e^{j\omega_{lmn}t}, \tag{4.1}$$

where A_{lmn} and ψ_{lmn} are constants, p is the acoustic pressure, J_m is the m^{th} order Bessel function, k is the wavenumber, t is the time, ω is the angular frequency, and l, m, and n are nonnegative integers with at least one nonzero. Additionally, $k_l = l\pi/h$ and $\omega_{lmn} = c\sqrt{k_{mn}^2 + k_l^2}$.

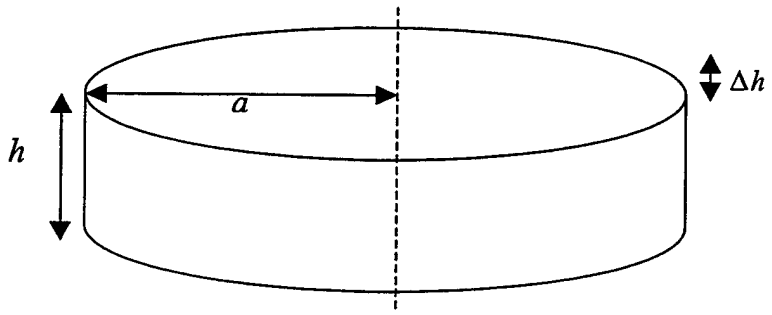

Figure 4.1. Height modulation of a cylindrical cavity.

B. ENERGY STORED IN THE FUNDAMENTAL RADIAL MODE

We will deal with the fundamental radial mode, which occurs for $l = 0$, $m = 0$, and $n = 1$. from Eq. (4.1), the pressure is given by

$$p_{001} = A_{001} J_o(k_{01} r) e^{j\omega_{001} t}, \tag{4.2}$$

where k_{01} is determined by the boundary condition at $r = a$ which is $\partial p/\partial r = 0$ or equivalently $u = 0$ for a rigid boundary. In terms of the Bessel functions, the boundary condition becomes $J_0'(k_{01}a) = -J_1(k_{01}a) = 0$. The velocity potential ϕ is related to the acoustic pressure by $p = -\rho_0 \partial\phi/\partial t$. Using this relationship and Eq. (4.2) yields the velocity potential for the fundamental radial mode

$$\phi_{001} = \left[\frac{jA_{001}J_0(k_{01}r)}{\rho_0 \omega_{001}}\right] e^{j\omega_{001}t}. \tag{4.3}$$

The gradient of the velocity potential gives the particle velocity u for the fundamental radial mode

$$u_{001} = \left[\frac{-jA_{001}J_1(k_{01}r)}{\rho_0 c} \right] e^{j\omega_{001}t}, \tag{4.4}$$

where the relationship $\omega_{001} = ck_{01}$ has been used to simplify the expression. The pressure and velocity amplitudes as functions of r are shown in Fig. 4.2.

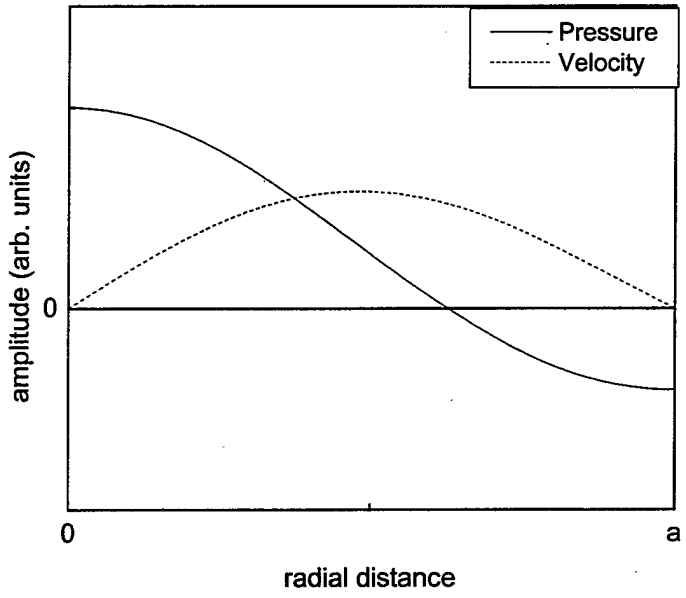

Figure 4.2. Profile of the fundamental radial mode of a cylindrical resonator.

The instantaneous energy density of an acoustic wave is given by

$$\mathcal{E} = \tfrac{1}{2}\rho_o \left[u^2 + \left(\frac{p}{\rho_0 c} \right)^2 \right]. \tag{4.5}$$

Substituting Eqs. (4.2) and (4.4) into Eq. (4.5), we find the instantaneous energy density of the fundamental radial mode to be

$$\mathcal{E} = \tfrac{1}{2}\rho_0 \left[\frac{A_{001}}{\rho_0 c} \right]^2 \left[J_0^2(k_{01}r)\cos^2 \omega t + J_1^2(k_{01}r)\sin^2 \omega t \right]. \tag{4.6}$$

The total energy E can be found by time averaging and integrating the instantaneous energy density over the cylinder volume:

$$E = \left(\frac{\rho_0}{4}\right)\left(\frac{A_{001}}{\rho_0 c}\right)^2 \int_0^h \int_0^{2\pi} \int_0^a \left[J_0^2(k_{01}r) + J_1^2(k_{01}r)\right] r dr d\phi dz$$

$$= \left(\frac{\pi h \rho_0}{2}\right)\left(\frac{A_{001}}{\rho_0 c}\right)^2 \int_0^a \left[J_0^2(k_{01}r) + J_1^2(k_{01}r)\right] r dr . \qquad (4.7)$$

Evaluating the integral of Eq. (4.7) and applying the boundary condition $J_1(k_{01}a) = 0$, yields:

$$\int_0^a \left[J_0^2(k_{01}r) + J_1^2(k_{01}r)\right] r dr = a^2 J_0^2(k_{01}a), \qquad (4.8)$$

where each term of the integrand contributes equally to the integral, which must be the case because the average kinetic energy equals the average potential energy. Substituting Eq. (4.8) into Eq. (4.7) yields

$$E = \left(\frac{\pi h \rho_0}{2}\right)\left(\frac{A_{001}}{\rho_0 c}\right)^2 a^2 J_0^2(k_{01}a). \qquad (4.9)$$

C. POWER DISSIPATION

Swift (1988) derives the following general expression for the average rate of energy dissipation $\dot{e}$ per unit of surface area of a resonator:

$$\dot{e} = \frac{1}{4}\frac{p^2}{\rho_0 c^2}\delta_\kappa(\gamma - 1)\omega + \frac{1}{4}\rho_0 u^2 \delta_\nu \omega, \qquad (4.10)$$

where δ_κ is the thermal penetration depth and δ_ν is the viscous penetration depth. Blackstock (2000) shows that the viscous penetration depth can be expressed as:

$$\delta_\nu = \sqrt{\frac{2\mu}{\omega\rho_0}}, \tag{4.11}$$

where μ is the coefficient of shear viscosity. Furthermore, the thermal penetration depth is related to the viscous penetration depth by the following relationship:

$$\delta_\kappa = \delta_\nu / \sqrt{\mathrm{Pr}}, \tag{4.12}$$

where Pr is the Prandtl number. Using Eq. (4.12), Eq. (4.10) becomes

$$\dot{e} = \frac{1}{4}\delta_\nu \omega \left[\frac{p^2}{\rho_0 c^2} \frac{(\gamma - 1)}{\sqrt{\mathrm{Pr}}} + \rho_0 u^2 \right]. \tag{4.13}$$

The rate of total energy dissipation $\dot{E}$ for the fundamental radial mode can be found by substituting the magnitude of Eqs. (4.2) and (4.4) for the pressure and velocity, respectively, and then integrating Eq. (4.13) over the surface area of the cavity:

$$\dot{E} = \frac{1}{4} \frac{A_{001}^2 \delta_\nu \omega}{\rho_0 c^2} \iint \left[\frac{\gamma - 1}{\sqrt{\mathrm{Pr}}} J_0^2(k_{01} r) + J_1^2(k_{01} r) \right] dS. \tag{4.14}$$

For the top and bottom of the cavity, the differential surface area element is $rdrd\theta$. The differential surface area element for the side is $ad\theta dz$. Integrating over the top and bottom and evaluating for the first radial mode yields

$$\int_0^{2\pi} \int_0^a \left[\frac{\gamma - 1}{\sqrt{\mathrm{Pr}}} J_0^2(k_{01} r) + J_1^2(k_{01} r) \right] r dr d\theta = \left(\frac{\gamma - 1}{\sqrt{\mathrm{Pr}}} + 1 \right) \pi a^2 J_0^2(k_{01} a). \tag{4.15}$$

Similarly, integrating over the side and evaluating for the first radial mode yields

$$\int_0^h \int_0^{2\pi} \left[\frac{\gamma - 1}{\sqrt{\mathrm{Pr}}} J_0^2(k_{01}a) + J_1^2(k_{01}a) \right] a d\theta dz = 2\pi a h \frac{\gamma - 1}{\sqrt{\mathrm{Pr}}} J_0^2(k_{01}a), \tag{4.16}$$

where $J_1(k_{01}a) = 0$. Losses at the side are solely thermal losses since the pressure is a maximum at the wall while the velocity is zero. Using the results from Eqs. (4.15) and (4.16), Eq. (4.14) becomes

$$\dot{E} = \frac{1}{4} \frac{A_{001}^2 \delta_v \omega}{\rho_0 c^2} \pi a J_0^2(k_{01}a) \left[\frac{\gamma - 1}{\sqrt{\mathrm{Pr}}} (a + 2h) + a \right]. \tag{4.17}$$

D. QUALITY FACTOR AND PARAMETRIC DRIVE THRESHOLD

The quality factor is related to the energy stored at resonance and the energy dissipation by the relationship $Q = \omega E / \dot{E}$. The energy stored at resonance is given by Eq. (4.9) while the rate of energy dissipation is given by Eq. (4.17). Thus,

$$Q = \frac{2ah}{\delta_v \left[\frac{\gamma - 1}{\sqrt{\mathrm{Pr}}} (a + 2h) + a \right]}. \tag{4.18}$$

Substituting Eq. (4.11) into Eq. (4.18) and converting the angular frequency into frequency yields

$$Q = \sqrt{\frac{\pi f \rho_0}{\mu}} \frac{2ah}{\left[(\gamma - 1)/\sqrt{\mathrm{Pr}} \right] (a + 2h) + a}. \tag{4.19}$$

Equation (4.19) is valid for the first radial mode of a cylindrical resonator, as long as the bulk losses are insignificant compared to the boundary layer thermoviscous losses.

The resonant frequency for the fundamental radial mode is given by

$$f_0 = c(3.830)/2\pi a \tag{4.20}$$

where $3.830/a$ is the wavenumber for the fundamental radial mode. As stated in Ch. II, the dimensionless parametric drive threshold η_{th} for a parametric drive, where the square frequency of a mode is modulated as $\omega_0^2(1+\eta\cos 2\omega_0 t)$, is given by $\eta_{th} = 2/Q$. Substituting Eqs. (4.19) and (4.20) into this expression yields the parametric drive threshold for the fundamental radial mode of the cylindrical cavity:

$$\eta_{th} = \sqrt{\frac{2\mu}{3.830\rho_0 c}}\frac{\left[(\gamma-1)/\sqrt{\mathrm{Pr}}\right](a+2h)+a}{h\sqrt{a}}. \tag{4.21}$$

E. MODULATING THE SPEED OF SOUND

One means of parametrically exciting the fundamental radial mode is to vary the speed of the sound in the cylindrical resonator. Compressing and expanding an enclosed gas causes its temperature to increase and decrease, respectively. If we treat the enclosed gas as an ideal gas and assume that the compression occurs adiabatically, then it is possible to relate the temperature change to the volume change. We consider using a driver to alternately expand and compress the gas. In order to achieve an approximately uniform temperature modulation, it is necessary to drive a piston at a frequency sufficiently below the resonant frequency of the fundamental longitudinal mode. Using Eqs. (3.1) and (4.20), and requiring that the drive frequency $2f_0$ be much less than the fundamental longitudinal frequency, we find that the cylinder height and radius are related by:

$$h \ll 0.4101a\,. \tag{4.22}$$

To evaluate the feasibility of parametrically exciting the fundamental radial mode, it is necessary to provide a further quantification of this restriction.

The particle velocity and pressure of an enclosed cylinder driven by a vibrating piston at $x = 0$ and rigidly terminated wall at $x = h$ are given by

$$p = -jZ_0 u_0 e^{j\omega t}\frac{\cos k(h-x)}{\sin kh}, \tag{4.23}$$

$$u = u_0 e^{j\omega t}\frac{\sin k(h-x)}{\sin kh}. \tag{4.24}$$

where Z_0 is the acoustical impedance, and u_0 is the amplitude of the particle velocity (Blackstock, 2000). The acoustic impedance of a short cylinder can be expressed in terms of the stiffness and inertia. For low frequency we can neglect the inertia, and the acoustic impedance is then $Z_0 = \rho_0 c$. Furthermore, for $kh \ll 1$ the expressions for the particle velocity and pressure can be written

$$p = -je^{j\omega t}\frac{Z_0 u_0}{kh} = \frac{u_0 \rho_0 c^2}{j\omega h}e^{j\omega t}, \tag{4.25}$$

$$u = u_0(1 - x/h)e^{j\omega t}. \tag{4.26}$$

Thus, we see that the pressure is approximately a constant inside the cavity and the velocity approximately decreases linearly from the maximum at the piston to zero at the end. These expressions are valid in the limit of $kh<<1$, which can be rewritten as

$$h \ll (0.1305)a\,, \tag{4.27}$$

for the case where the drive frequency is twice the fundamental radial mode frequency. Eq. (4.27) is more restrictive than Eq. (4.22) for the case of parametrically exciting the radial mode.

Figure 4.3 shows the pressure variation in a cylindrical cavity as a function of the wavelength. As the value of *kh* decreases, Figure 4.3 shows that the normalized pressure approaches a uniform value. The pressure is a maximum at the end opposite the driver. For the purposes of this analysis, we assume that the cylinder height is a tenth of the wavelength ($h = \lambda/10$). This relationship can be rewritten by applying the boundary condition at the wall for the fundamental radial mode ($k = 3.830/a$) to yield

$$h = 0.16a. \tag{4.28}$$

While appearing to violate Eq. (4.27), this provides a fairly uniform pressure distribution in the cylinder without being too restrictive.

The wavelength of the fundamental radial mode is determined by the radius of the cylinder. The frequency of the fundamental radial mode is dependent on the wavelength and the speed of sound. Thus, by varying the speed of sound at twice the frequency of the fundamental radial mode, it may be possible to parametrically excite the fundamental radial mode. We now determine the variation of the speed of sound.

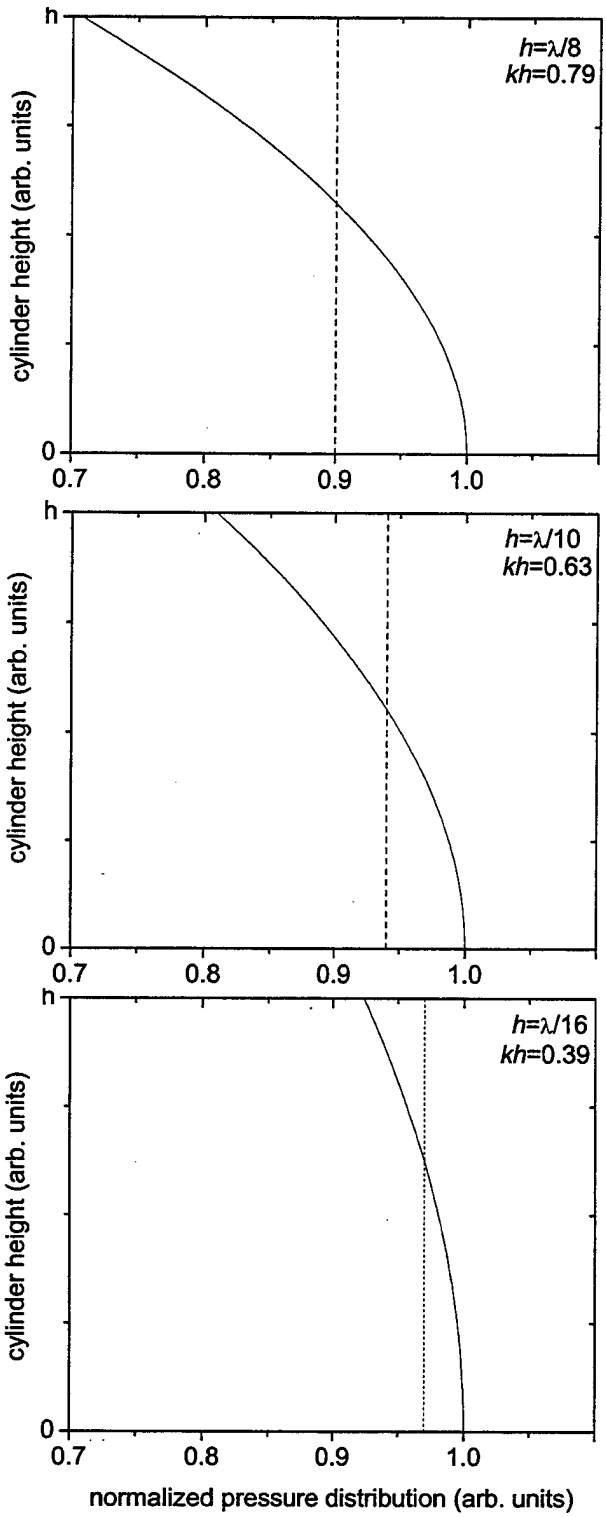

Figure 4.3. Normalized pressure distributions for various drive frequencies as a function of the cylindrical cavity height. (Dashed lines indicate the average pressure).

The first law of thermodynamics can be expressed as

$$dE = dQ - PdV \tag{4.29}$$

for one mole of gas, where dE is the differential internal energy, dQ is the heat absorbed, dV is the differential volume of the gas, and P is the pressure. If we consider an infinitesimal quasistatic process in which the temperature changes by dT, then the internal energy can be expressed as

$$C_v dT = dQ - PdV\,, \tag{4.30}$$

where C_v is the molar heat capacity at constant volume. Furthermore, if we consider an ideal gas that is adiabatically isolated so that it absorbs no heat, then $dQ = 0$ and $PV = \mathcal{R}T$, where $\mathcal{R}$ is the universal gas constant. Eq. (4.30) then becomes

$$\frac{C_v}{\mathcal{R}}\frac{dT}{T} = -\frac{dV}{V}\,, \tag{4.31}$$

An equivalent derivation of Eq. (4.31) can be done using the ideal gas law and the pressure-volume relationship for an adiabatic process ($PV^{\gamma} = \text{constant}$).

The speed of sound in a medium is given by the following relationship:

$$c = \sqrt{\gamma r T}\,, \tag{4.32}$$

where γ is the ratio of heat capacities, r is the specific gas constant, and T is the temperature in degrees Kelvin. Since the angular frequency ω of a mode is proportional to the sound speed c and the sound speed is proportional to the square root of the absolute temperature T, then

$$\omega^2 = \omega_0^2\left(1+\frac{\Delta T}{T}\cos 2\omega t\right), \tag{4.33}$$

where ΔT is the peak amplitude of the temperature modulation. Thus, the dimensionless parametric drive amplitude is given by $\eta = \Delta T / T$.

Since the cylinder volume is modulated by varying the height, then

$$\frac{\Delta V}{V} = \frac{\Delta h}{h}. \tag{4.34}$$

Eq. (4.34) can be substituted into Eq. (4.31) and rearranged to yield

$$\frac{\Delta T}{T} = -(\gamma - 1)\frac{\Delta h}{h}, \tag{4.35}$$

where we have also made use of the relationship: $\mathcal{R}/C_v = \gamma - 1$. We now have an expression for the dimensionless parametric drive amplitude η:

$$\eta = -(\gamma - 1)\frac{\Delta h}{h}. \tag{4.36}$$

We now desire to express the threshold of the modulated parameter in terms of the geometrical and physical properties of the resonator. Recall that the dimensionless parametric threshold is related to the quality factor of a mode by $\eta_{th} = 2/Q$. Thus, Eq. (4.21) can be substituted into Eq. (4.36) and rearranged to yield

$$\Delta h = \sqrt{\frac{2\mu}{3.830\rho_0 c}}\frac{1}{\sqrt{a}}\left(\frac{a+2h}{\sqrt{\mathrm{Pr}}}+\frac{a}{\gamma-1}\right). \tag{4.37}$$

Eq. (4.37) gives the required amplitude of the driver displacement to parametrically excite the fundamental radial mode of a cylindrical resonator. It is interesting to note that

a gas with a specific heat ratio of approximately unity will have a large threshold value regardless of the other parameters. This occurs because $\gamma = 1$ corresponds to isothermal volume changes. [Refer to Eq. (4.36).]

F. EFFECTS OF USING VARIOUS GASES IN THE CYLINDRICAL CAVITY

If we now consider the use of various gases in the cylindrical resonator, Eq. (4.37) becomes

dry air: $$\Delta h = \frac{5.654\times10^{-4}a + 3.643\times10^{-4}h}{\sqrt{a}}, \tag{4.38}$$

helium: $$\Delta h = \frac{6.747\times10^{-4}a + 6.013\times10^{-4}h}{\sqrt{a}}, \tag{4.39}$$

SF_6: $$\Delta h = \frac{1.161\times10^{-3}a + 2.056\times10^{-4}h}{\sqrt{a}}, \tag{4.40}$$

CO_2: $$\Delta h = \frac{5.741\times10^{-4}a + 2.898\times10^{-4}h}{\sqrt{a}}, \tag{4.41}$$

where the cylinder height h and radius a are in units of meters. The thermodynamic and fluid properties for these gases are compiled in Table 1 of Appendix A. Equations (4.38) through (4.41) give the threshold drive amplitude necessary to parametrically excite the fundamental radial mode of a cylindrical resonator. The equations are plotted in Fig. 4.4 for a cylindrical cavities with 10 cm and 20 cm radius. SF_6 is disadvantageous due to its ratio of specific heats being near unity $(\gamma = 1.09376)$. Figures 4.5, 4.6, and 4.7 show

level curves of the threshold drive amplitude. Also included on Fig. 4.5, 4.6, and 4.7 is a line depicting the relationship between the drive frequency and the height of the cylindrical cavity. We require that the height of the cylindrical cavity be less than one-tenth the wavelength of the driver to ensure a relatively uniform pressure distribution.

As for the straight pipe, it is worthy to note the quality factors for these different gases. For a cylindrical cavity of 20 cm radius and 1.0 m height , the quality factor Q is 4700 for air, 7500 for CO_2. and 1800 for He. The quality factor is approximately inversely proportional to the square root of the cylinder radius. Thus, decreasing the radius by half will increase the Q by approximately a factor of 1.4.

Figures 4.8 and 4.9 show the threshold amplitude of the parametric drive for a cylindrical cavity with heights of 1.0 or 2.0 cm and filled with either helium, air, carbon dioxide, or sulfur hexafluoride. Also shown on Fig. 4.8 and 4.9 are the displacement amplitudes of various drivers, where the cylinder radius is chosen to equal the driver radius. The driver corresponding to each point in these figures can be determined from the data compiled in Appendix C. As with the closed pipe, the EVX-150A generated the largest amplitude for a given gas. However, the displacement produced by all of these drivers is substantially below the threshold necessary to parametrically excite the fundamental radial mode. We conclude that such excitation is infeasible, at least for the drivers we considered.

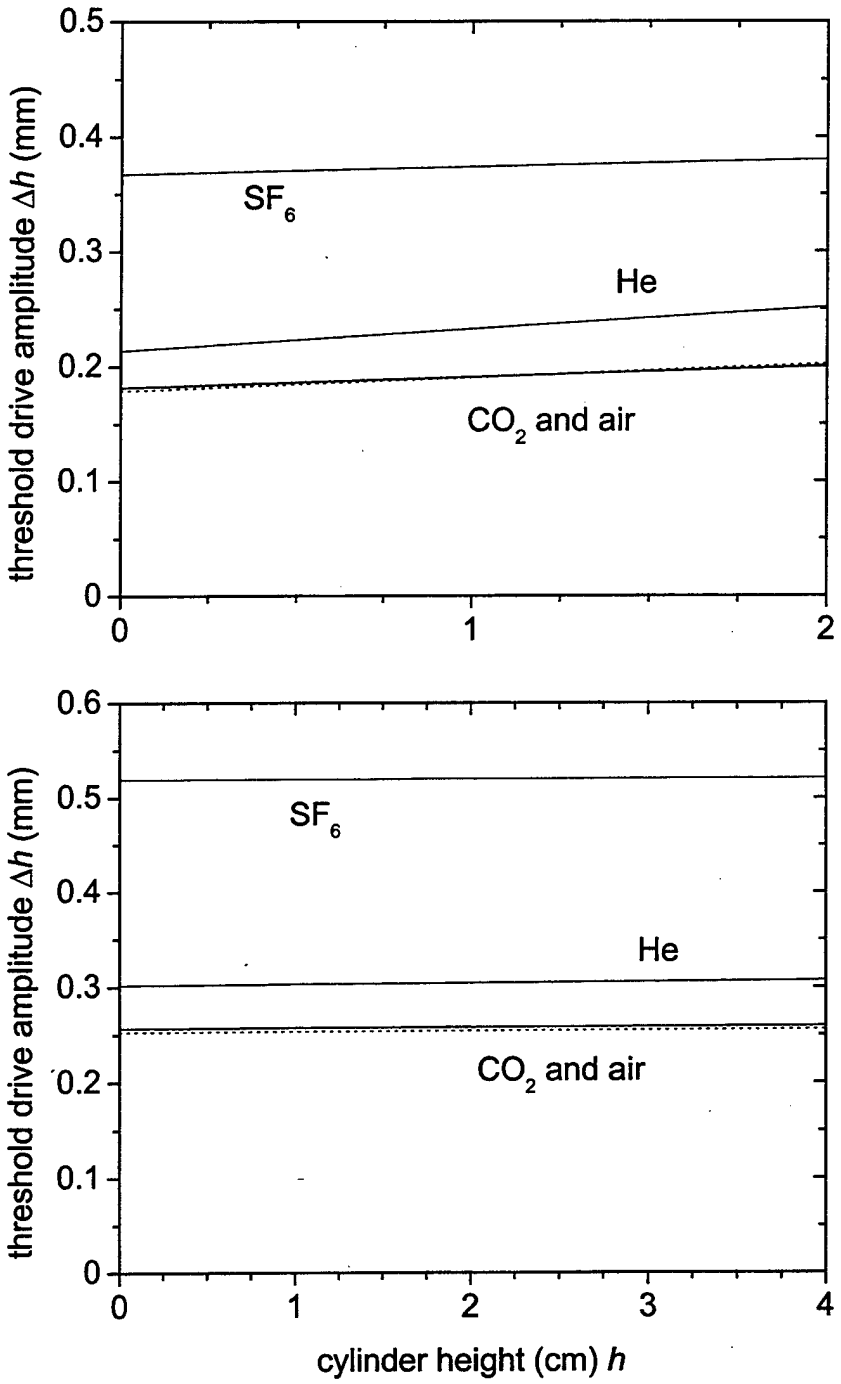

Figure 4.4. Threshold drive amplitude for a cylindrical cavity with a 10 cm radius (top) and a 20 cm radius (bottom). Air is indicated by the dotted line while carbon dioxide is indicated by the solid line.

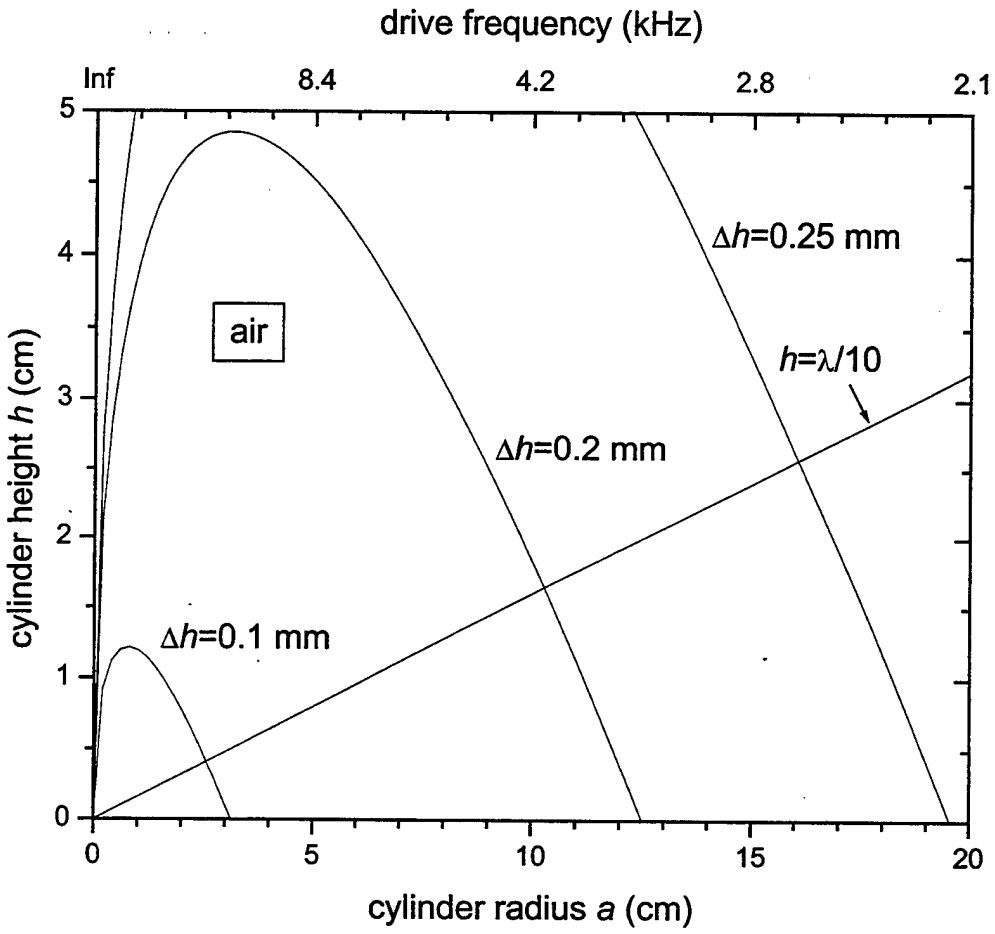

Figure 4.5. Level curves of the parametric drive threshold for the fundamental radial mode of an air filled cylindrical cavity at 25 °C and 1 atm.

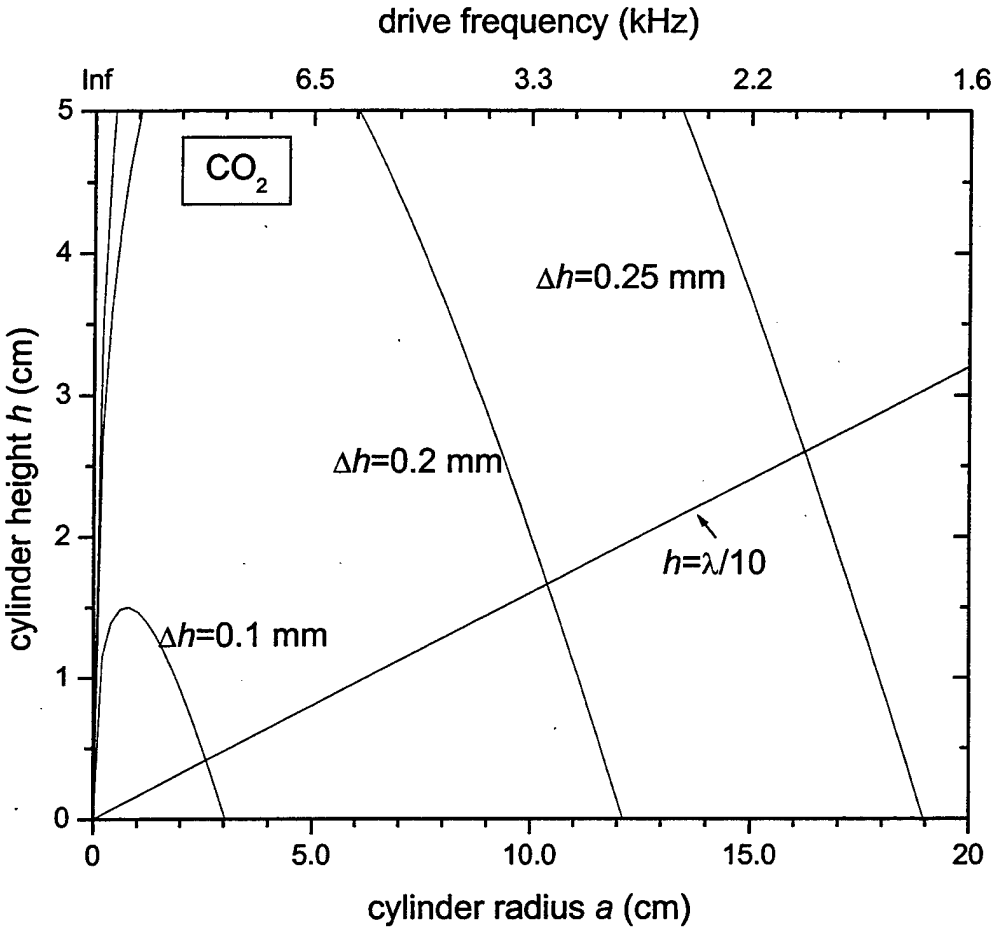

Figure 4.6. Level curves of the parametric drive threshold for the fundamental radial mode of a carbon dioxide filled cylindrical cavity at 25 °C and 1 atm.

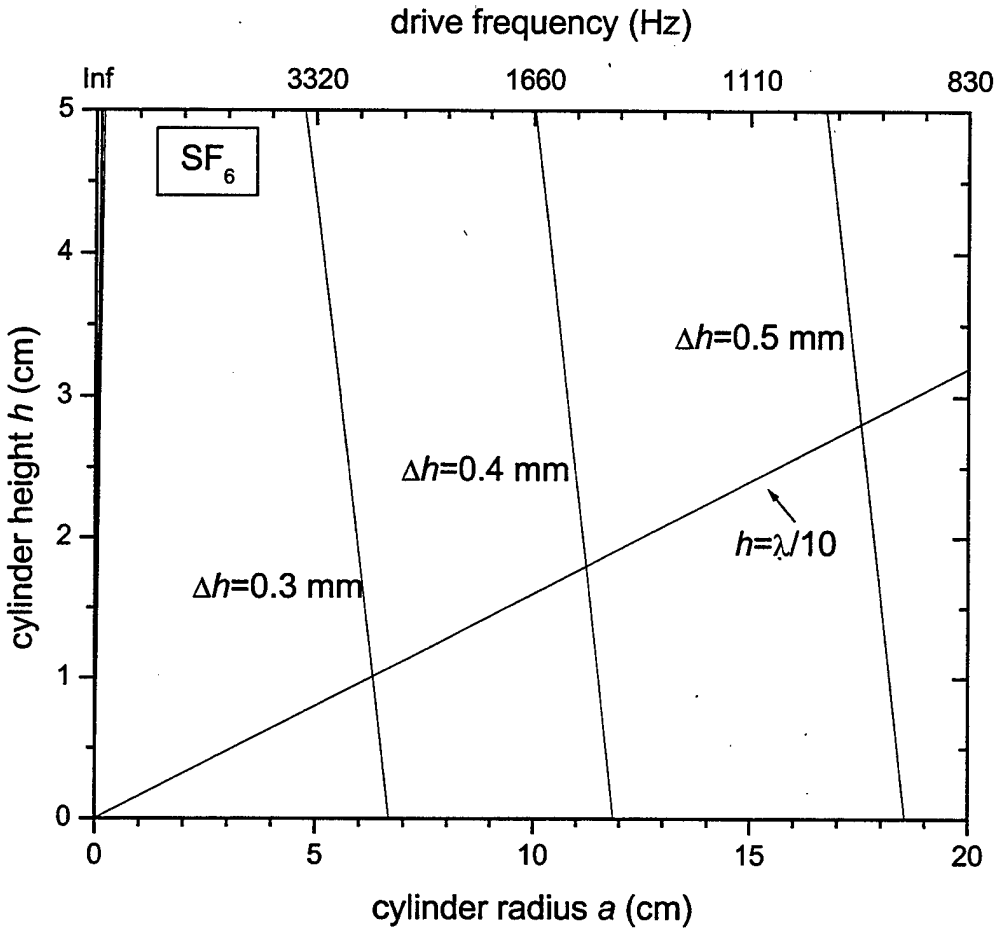

Figure 4.7. Level curves of the parametric drive threshold for the fundamental radial mode of a sulfur hexafluoride filled cylindrical cavity at 25 °C and 1 atm.

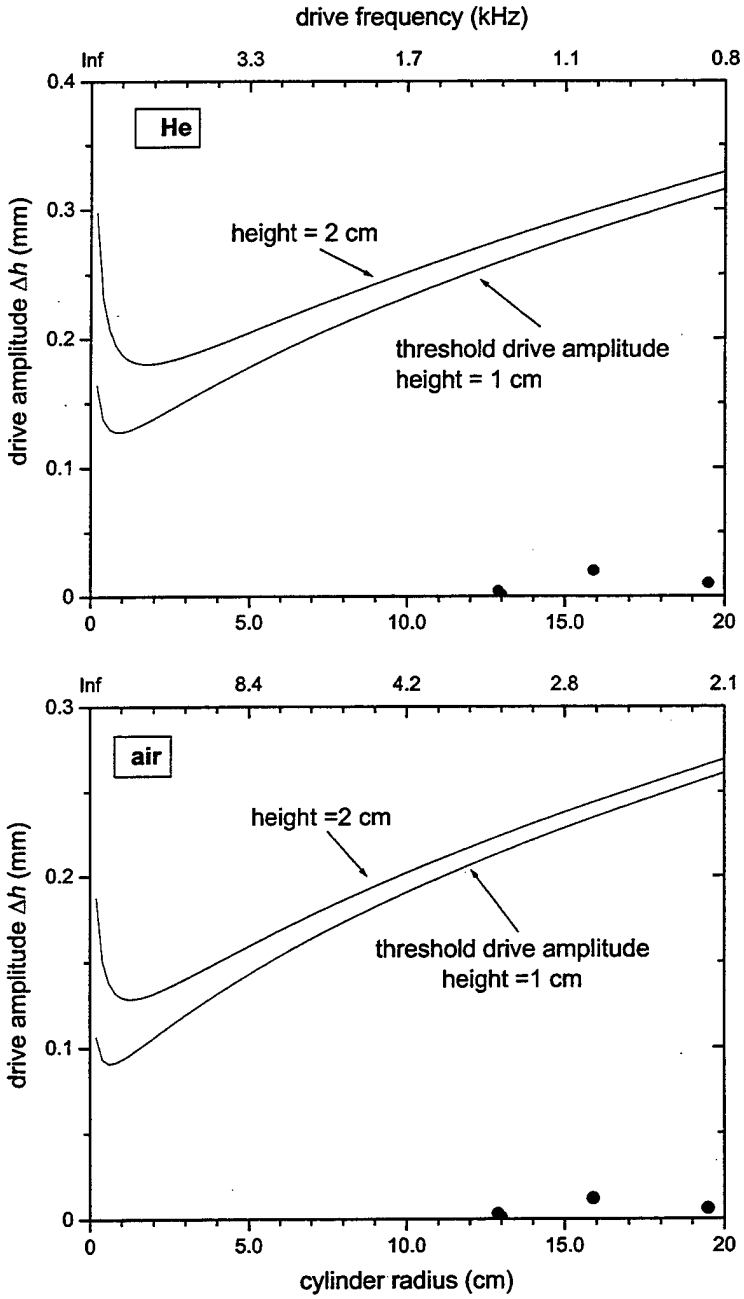

Figure 4.8. Threshold drive amplitude (curves) and various driver amplitudes (points) for a given cylindrical cavity geometry and filled with helium (top) or air (bottom).

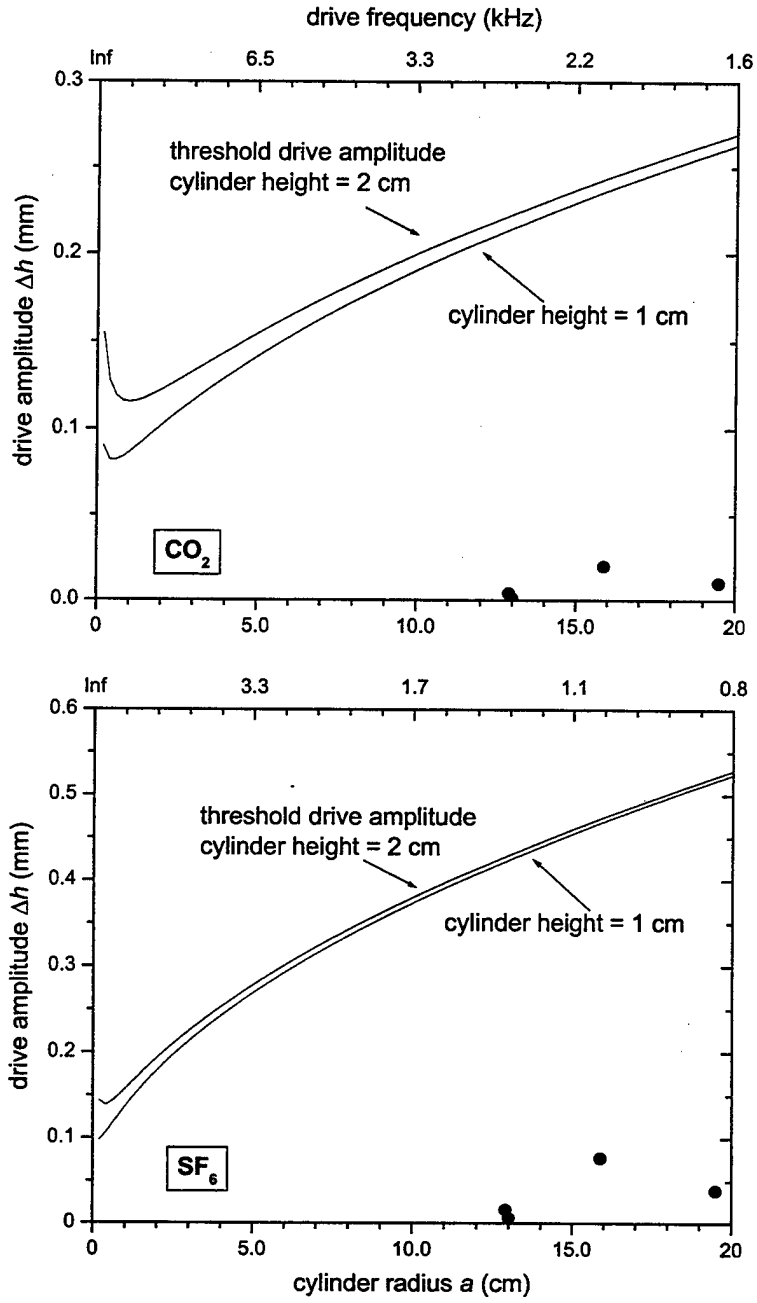

Figure 4.9. Threshold drive amplitude (curves) and various driver amplitudes (points) for a given cylindrical cavity geometry and filled with carbon dioxide (top) or sulfur hexafluoride (bottom).

V. TEMPERATURE MODULATION BY ELECTROMAGNETIC RADIATION

In addition to the geometrical modulation of the temperature of a fluid in an acoustic resonator considered in Ch. IV, another possibility is to subject the fluid to electromagnetic radiation whose intensity is modulated. This is more complicated to understand and calculate, but may be more practical. In this chapter, we consider temperature modulation of the fluid in a resonator by an electromagnetic wave source, which may be a modulated magnetron (Fig. 5.1).

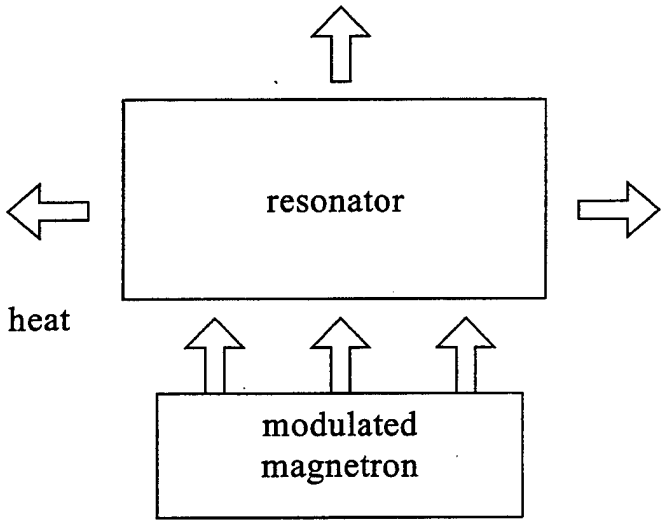

Figure 5.1. Schematic arrangement for microwave modulation of the temperature of the fluid in an acoustic resonator.

A. QUALITATIVE DESCRIPTION

The time variation of the power output of a modulated electromagnetic wave source is typically an on-off cycle shown in Fig. 5.2(a). The modulation occurs at acoustic frequencies, specifically, twice the natural frequency of the acoustic mode to be parametrically excited. We assume that the radiation is distributed uniformly over the fluid of the resonator. The fluid is expected to absorb the radiation at a rate proportional to the intensity, regardless of the temperature. (We assume that the temperature is not sufficiently high that ionization of the fluid occurs.)

Figure 5.2(b) shows a sketch of the spatially-averaged temperature of the gas for short times after the source is turned on. The temperature T_o is the constant temperature of the walls of the resonator. The temperature of the gas increases approximately linearly during the on-time of the source, and the temperature decreases a very small amount during the off-time. This behavior occurs because the on and off times are short, and because the temperature of the fluid is only a small amount greater than T_o, so the heat flow through the walls is small.

As the temperature of the fluid increases, the rate of heat flow increases. This produces two effects: the temperature will not rise as rapidly during the on-time, because some heat flows out of the system, and the temperature will drop more rapidly during the off-time, due to the greater temperature gradient and thus greater heat flow. Eventually the temperature of the fluid will become sufficiently large that the system will be in steady state, which is sketched in Fig. 5.2(c). In this case, the net gain in heat during the on-time equals the heat lost during the off-time. It should be noted that the peak-to-peak

amplitude of the temperature oscillations in the steady state is less than the change in temperature during the on-time for short times [Fig. 5.2(b)]. That is, the temperature oscillations tend to "wash out." This is disadvantageous because the amplitude of the temperature oscillations must be greater than a threshold value if parametric excitation is to occur. The greater the source power P, the greater will be the operating temperature T_{av} and the amplitude of the temperature oscillations. Hence, parametric excitation should occur if T_{av} is sufficiently large.

It is not difficult to obtain a powerful magnetron and to modify it so that the power can be modulated at acoustic frequencies (Lamb, 2000). The problem is that the requisite operating temperature T_{av} may be prohibitively large. For example, the fluid may change its state, including possible ionization. As another example, convection could occur, which would cause turbulence and thus lower the quality factor of the acoustic mode.

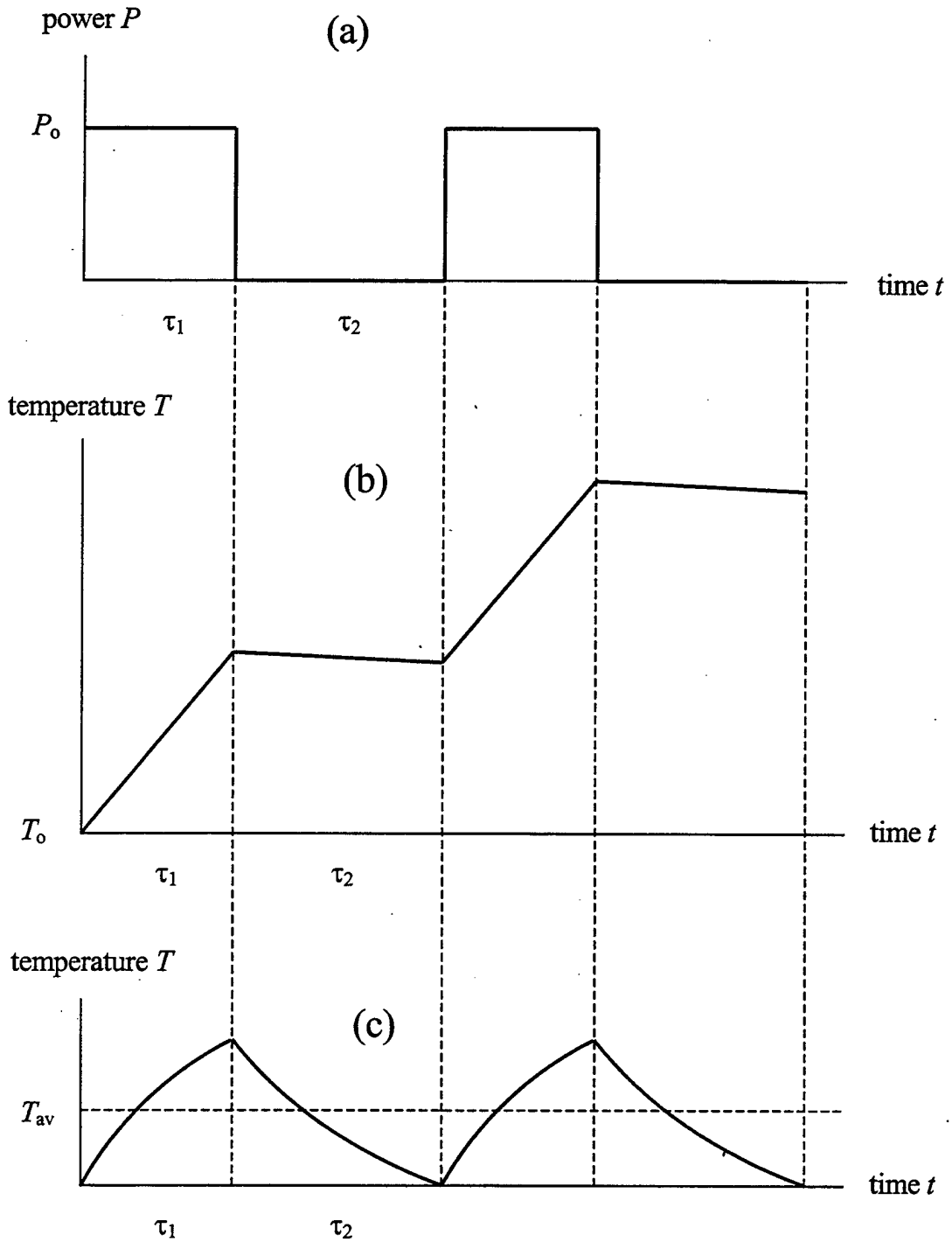

Figure 5.2. Time behavior of (a) the power delivered by the microwave source, and the spatially-averaged temperature of the fluid (b) for short times and (c) in the steady state.

B. GENERAL FORMULATION OF PROBLEM

If $T(\vec{r},t)$ is the temperature of a substance and κ is the thermal conductivity, the heat flux is

$$\vec{q} = -\kappa \vec{\nabla} T, \tag{5.1}$$

which is measured in energy per unit area per unit time. Conservation of energy yields the continuity law (Landau and Liftshitz, 1959)

$$\rho c_p \frac{\partial T}{\partial t} + \vec{\nabla} \cdot \vec{q} = g, \tag{5.2}$$

where ρ is the density (which is not necessarily constant), c_p is the specific heat at constant pressure, and $g(\vec{r},t)$ is the heat source function, which is measured in energy per unit volume per unit time.

We consider the case of the absorption of electromagnetic radiation that is uniformly distributed over a confined fluid. The heat source function g is proportional to the density ρ, and the integral of g over the total volume V of the substance must yield the total power P of the absorbed electromagnetic waves, so $g = P\rho / M$, where M is the total mass of the gas. If the average density of the fluid is ρ_o (which is the ambient density), then $g = P\rho / \rho_o V$.

The boundary condition is that the temperature is constant on all nonadiabatic surfaces. We express this as

$$T\big|_{boundary} = T_o. \tag{5.3}$$

We first consider a liquid (e.g., water). Because the thermal conductivity κ and density ρ are approximately independent of temperature, the elimination of the heat flux in Eqs. (5.1) and (5.2) yields the equation

$$\frac{\partial T}{\partial t} = \sigma \nabla^2 T + \psi, \tag{5.4}$$

where the thermal diffusivity is the constant $\sigma = \kappa / \rho_0 c_p$, and the temperature source function is the spatial constant $\psi = g / \rho c_p = P / V \rho_0 c_p$.

To show how Eq. (5.4) can be solved, we decompose the temperature source function and the temperature into time-averaged and oscillatory parts (whose time averages are zero):

$$\psi = \overline{\psi} + \psi'(t), \tag{5.5}$$

$$T = \overline{T}(\vec{r}) + T'(\vec{r}, t), \tag{5.6}$$

where the overbars denote time-averaged quantities. The boundary conditions are

$$\overline{T}\big|_{boundary} = T_o \text{ and } T'\big|_{boundary} = 0. \tag{5.7}$$

By substituting expressions (5.5) and (5.6) into Eq. (5.4), and recognizing that the time-averaged and oscillatory quantities must separately satisfy the equation, we have

$$\nabla^2 \overline{T} = -\overline{\psi} / \sigma, \tag{5.8}$$

$$\frac{\partial T'}{\partial t} = \sigma \nabla^2 T' + \psi'. \tag{5.9}$$

The time-averaged equation (5.8) is Poisson's equation, which also arises in electrostatics. The solution of this is considered in the next section. In the oscillatory equation (5.9), we assume a sinusoidally-varying source function by letting $\psi' \to \psi' \exp(i\omega t)$, where ψ' is now an amplitude and where the real part is understood. Letting $T' \to T' \exp(i\omega t)$ gives

$$\sigma \nabla^2 T' - i\omega T' = -\psi' . \tag{5.10}$$

The particular solution is $T' = \psi' / i\omega$. For a cylindrical geometry, the homogeneous solution is a Bessel equation of zero order with a complex argument which is neither purely real nor purely imaginary.

The situation is substantially more complicated for gases. For an ideal gas, the thermal conductivity is $\kappa = \alpha T^{1/2}$, where α is independent of temperature. Furthermore, the density varies as $\rho = \beta / T$, where β is a spatial constant given by $\beta = pm/k$, where p is the pressure, m is the molecular mass, and k is Boltzmann's constant. The pressure can be determined self-consistently by demanding that the total mass (volume integral of the density) equal the total mass of the gas. Eliminating the heat flux from Eqs. (5.1) and (5.2), then yields

$$\frac{\partial T}{\partial t} = \zeta T^{3/2} \nabla^2 T + \zeta T^{1/2} \left(\vec{\nabla} T \right) + \psi , \tag{5.11}$$

where $\psi = g / \rho c_p = P / V \rho_0 c_p$ as before, and $\zeta = \alpha / \beta c_p$.

The above procedure with the time-averaged and oscillatory parts can now be followed. The time-averaged equation is highly nonlinear, and its solution would

probably have to be accomplished numerically. The oscillatory equation is a linear equation because we assume small temperature oscillations ($|T'| \ll \overline{T}$), and thus should be solvable. However, we roughly estimate in Sec. D that the operating temperature required for parametric excitation appears to be too high to be feasible. A high temperature would cause convection to occur, which is entirely omitted in the above analysis, and which is much more difficult to calculate. We thus leave the temperature calculations for future work, if the situation alters such that the calculations become worthwhile to do.

C. SPATIAL DISTRIBUTION OF THE STEADY-STATE TIME-AVERAGED TEMPERATURE

As explained in Sec. A, the time-averaged temperature must necessarily be elevated compared to the outside temperature. This occurs because an electromagnetic radiation drive cannot remove heat. The removal must be accomplished by conduction to the walls of the resonator, which are assumed to be maintained at a constant (e.g., room) temperature T_0. In this section, we determine a relationship that allows the operating temperature distribution of water in a resonator to be estimated.

It is instructive to begin with the one-dimensional case [Fig. 5.3(a)]. Note that this is identical to the two-dimensional case of a rectangle [Fig. 5.3(b)] if the walls at $y = 0$ and $y = b$ are adiabatic. The general solution of Poisson's equation (5.8) is

$$\overline{T} = Ax + B - \frac{\overline{\Psi}}{2\sigma} x^2 . \tag{5.12}$$

The boundary condition $T = T_0$ at $x = 0$ implies that $B = T_0$. The condition $T = T_0$ at $x = L$ then implies $A = \bar{\psi}L/2\sigma$. Hence, the solution is

$$\bar{T} = T_o + \frac{\bar{\psi}}{2\sigma} x(L - x). \tag{5.13}$$

The maximum temperature difference, which occurs at $x = L/2$, is $\Delta T_{max} = \bar{\psi}L^2/8\sigma$. The average temperature over the length of the resonator is $T_{av} = T_0 + \bar{\psi}L^2/12\sigma$. From Eq. (5.1), the outward heat flux at either boundary is $q = \bar{\psi}L/2$, which is independent of σ. This second result is obvious from energy conservation: In the gas, the source generates power per unit cross-sectional area equal to $\bar{\psi}L$. In the steady state, this must equal the total outward heat flux, which is twice the flux at each wall, so this flux must be $\bar{\psi}L/2$.

We next consider the two-dimensional case of a rectangle [Fig. 5.3(b)] all of whose walls are at temperature T_0. The assumption of a separated solution, $\bar{T}(x,y) = X(x)Y(y)$ yields

$$\frac{X''}{X} + \frac{Y''}{Y} = -\frac{\bar{\psi}}{\sigma}\frac{1}{XY}. \tag{5.14}$$

Due to the source term, this is not separable. This problem arises for any geometry of more than one dimension if the temperature has more than one degree of freedom; for example, a cylinder [Fig. 5.3(c)] all of whose walls are held at a fixed temperature T_0. Such problems can be solved by the Green's function method. The Green's function for the case of the cylinder is known (Jackson, 1975). The temperature distribution can then

be found by simply integrating the Green's function over the volume of the cylinder, because our source function is a constant.

There is another aspect to consider, however. The steady-state temperature distribution alters the speed of sound, which will distort the pressure and velocity distributions of a mode. This was responsible for the conclusion of Raspet *et al.* (1996) that a longitudinal acoustic mode in a pipe cannot be parametrically excited by electromagnetic radiation, because motion transverse to the resonator would occur. In the case of a radial mode of a cylinder, we can eliminate this problem by arranging the top and bottom surfaces [$z = 0$ and $z = h$ in Fig. 5.3(c)] to be adiabatic. The temperature distribution then does not cause the wave fronts to bend, but simply alters the speed. As we show below, this arrangement has the added advantage that there is only a single degree of freedom, so that the temperature distribution is easily determined.

For a cylinder with adiabatic top and bottom surfaces, Poisson's equation (5.8) reduces to the radially symmetric case

$$\frac{1}{r}\frac{d}{dr}\left(r\frac{d\overline{T}}{dr}\right)=-\frac{\overline{\Psi}}{\sigma}, \tag{5.15}$$

which has the general solution

$$\overline{T}=A\ln\left(\frac{r}{R}\right)+B-\frac{\overline{\Psi}}{4\sigma}r^2. \tag{5.16}$$

The boundary condition that the temperature remain finite at $r = 0$ yields $A = 0$. The boundary condition that the temperature equals T_0 at $r=a$ then yields $B=T_0+\overline{\Psi}a^2/4\sigma$. The solution is thus

$$\bar{T} = T_o + \frac{\bar{\Psi}}{4\sigma}\left(a^2 - r^2\right), \tag{5.17}$$

which is parabolic just as in the Cartesian one-dimensional result (5.13). The maximum temperature difference, which occurs between $r = 0$ and $r = a$, is

$$\Delta T_{\max} = \frac{\bar{\Psi} a^2}{4\sigma}. \tag{5.18}$$

From Eq. (5.17), we find that the average temperature over the volume of the resonator is

$$T_{av} = T_o + \frac{\bar{\Psi} a^2}{8\sigma}. \tag{5.19}$$

From Eq. (5.1), the outward heat flux at the radial boundary is

$$q = \frac{\bar{\Psi} a}{2}, \tag{5.20}$$

As in the Cartesian case, Eq. (5.20) is obvious from energy conservation: The source generates power in the gas equal to $\bar{\Psi}\pi a^2 h$, which in the steady state must equal the outward heat flux integrated over the side wall, which is $2\pi a h q$. Hence, $q = \bar{\Psi} a / 2$.

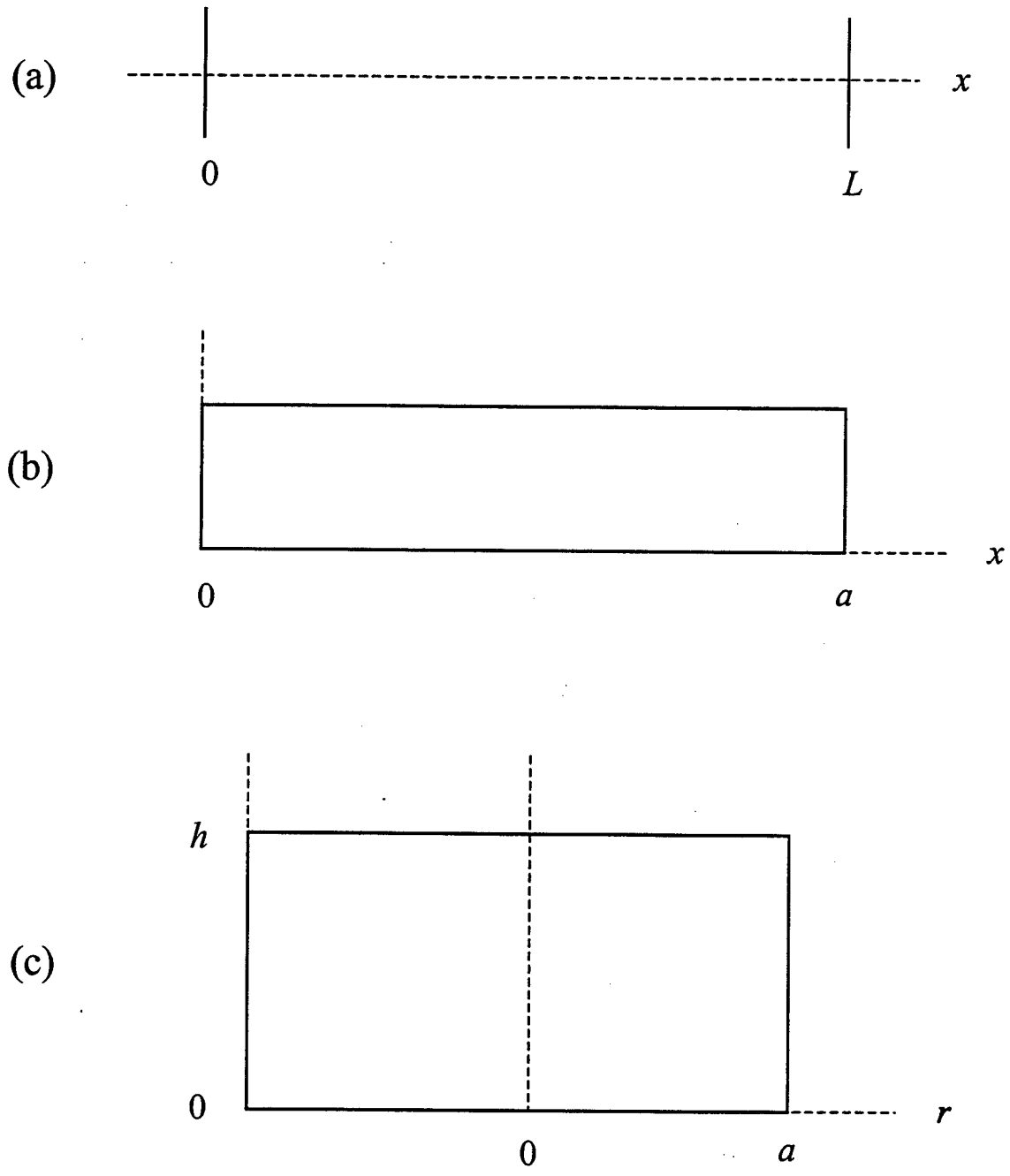

Figure 5.3. Various geometries of a resonator whose fluid is temperature-modulated by electromagnetic radiation: (a) one-dimensional case, (b) rectangle, and (c) cylinder.

D. HEAT LOSS DUE TO THERMAL CONDUCTION

For microwave modulation of the temperature, the source provides a heat input on the first part of the acoustic cycle. In the steady state, the net heat absorbed must equal the heat lost during the second part of the cycle. For an assumed operating temperature, we now estimate the time required for the temperature drop to occur. The peak to peak temperature drop must exceed twice the threshold temperature change in order for parametric excitation to occur.

The heat equation without generation can be written as:

$$\nabla^2 T = \frac{\rho_0 c_p}{\kappa} \frac{\partial T}{\partial t}, \tag{5.21}$$

The quantity $\kappa/\rho_0 c_p$ is often written as σ, and is called the thermal diffusivity. As explained in Sec. B, Eq. (5.21) does not apply to gases. However, it is expected to be a rough approximation if an average value of the thermal conductivity is used. If we now consider a cylinder in which the temperature is only radially dependent, then Eq. (5.21) becomes

$$\frac{1}{r}\frac{\partial}{\partial r}\left(r\frac{\partial T}{\partial r}\right) = \frac{1}{\sigma}\frac{\partial T}{\partial t}, \tag{5.22}$$

where r is the radial distance. We can also impose the following boundary and initial conditions:

$$T(a,t) = T_0, \tag{5.23}$$

$$T(r,0) = f(r), \tag{5.24}$$

where a is the cylinder radius, and $f(r)$ is the temperature distribution at time $t = 0$. It should be noted that this problem assumes that the cylinder end caps are adiabatically isolated (i.e. no heat flow occurs), as discussed in Sec. C. This problem has been solved in a number of textbooks on partial differential equations and we state the result from Powers (1987):

$$T(r,t) = T_0 + \sum_{n=1}^{\infty} b_n J_0(j_{0n} r/a) \exp\left(-j_{0n}^2 \sigma t / a^2\right), \tag{5.25}$$

where b_n are constants, J_0 is the zeroth order Bessel function, and j_{0n} are the zeros of J_0. The coefficients b_n can be found by applying the initial condition (Eq. (5.24)). Since the density and thermal conductivity are functions of the temperature, the thermal diffusivity is also temperature dependent. Equation (5.25) assumes that the thermal diffusivity is essentially constant over the range of temperatures in the cylinder.

For a cylindrical cavity subjected to a uniform heat source, the steady state temperature profile is parabolic in the case of water (Sec. C), and will be roughly parabolic for gases. We assume that the temperature profile is given by $T = T_0 + T_{\max}[1-(r/a)^2]$, where $T_{\max}$ is the temperature at the center of the cylinder. For ease of calculation, we will assume that the temperature profile can be approximated by the zeroth order Bessel function. Specifically, the temperature profile can be approximated by $T = T_0 + (1.09T_0) J_0(j_{01} r/a)$, where j_{01} is the first zero of J_0. This expression for the temperature fits the boundary condition at the wall and provides the same average temperature as the parabolic expression. Figure 5.4 shows a comparison of these two temperature profiles.

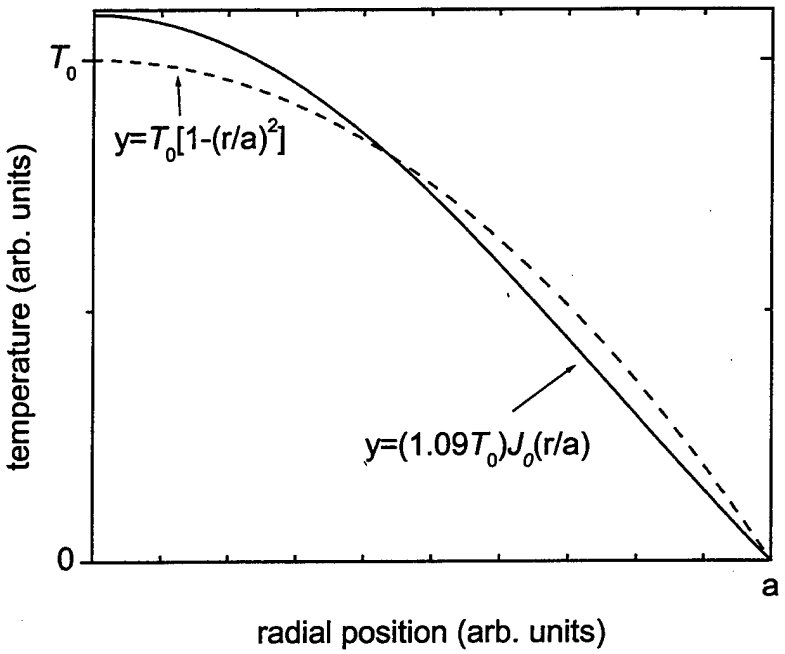

Figure 5.4. Temperature profile comparison for a cylinder with uniform heat generation.

Using the Bessel function approximation for the temperature, Eq. (5.24) becomes

$$T(r,0) = T_0 + (1.09T_0)J_0(j_{01}r/a). \tag{5.26}$$

From this initial condition, we can now determine the coefficients b_n. Substituting Eq. (5.26) into Eq. (5.25) yields

$$(1.09T_0)J_0(j_{01}r/a) = \sum_{n=1}^{\infty} b_n J_0(j_{0n}r/a). \tag{5.27}$$

From Eq. (5.27), we can see that the coefficients b_n all vanish, with the exception of n = 1. Thus, we see that $b_1 = 1.09T_{\max}$. The solution for the transient heat conduction problem now reduces to

$$T(r,t) = T_0 + T_{\max}' J_0(j_{0n} r/a) \exp\left(-j_{0n}^2 \sigma t/a^2\right), \tag{5.28}$$

where $T_{\max}' = 1.09 T_{\max}$. Equation (5.28) can be rearranged to determine the time for the temperature change to occur:

$$t = -\left(\frac{a^2}{j_{0n}^2 \sigma}\right) \ln\left(\frac{T(r,t) - T_0}{T_{\max}' J_0(j_{0n} r/a)}\right). \tag{5.29}$$

We now consider the case of a cylindrical cavity, with 20 cm radius and 50 cm height, filled with air and $T_{\max}' = 100$ °C. The threshold temperature change to parametrically excite the fundamental radial mode can be determined from Ch. IV (Eq. (4.21) where $\eta_{th} = \Delta T/T$). The values for the physical and thermal properties are contained in Appendix A. The threshold is $\Delta T = 0.225$ °C for a cylindrical cavity with a 20 cm radius and 50 cm height. The peak to peak temperature change is twice the value of the threshold ΔT. From Eq. (5.29), we find that the time for the temperature to drop by 0.450 °C is 255 ms. If the temperature drop occurs over half the drive cycle, then this corresponds to a drive frequency of 1.96 Hz. The parametric drive frequency required to parametrically excite the fundamental radial mode is 2.4 kHz. Thus, we see that the maximum drive frequency for this specific case is three orders of magnitude below the required drive frequency.

A similar calculation for a cylindrical cavity filled with carbon dioxide (same geometrical dimensions and temperature) gives the threshold $\Delta T = 0.162$ °C. The time for the peak to peak temperature drop to occur is 346 ms, which corresponds to a 1.45 Hz

drive frequency. The required drive frequency for this case is 1.8 kHz. Once again, we are three orders of magnitude below the required drive frequency.

From these calculations, it does not appear that the necessary heat transfer can occur over an acoustic cycle. A higher rate of heat transfer occurs for higher thermal gradients. However, in order to obtain a drive frequency near the required value, we would have to increase the temperature in the cylindrical cavity substantially beyond 100 °C. Thus, our analysis indicates that parametric excitation by microwave modulation of the temperature is not feasible.

THIS PAGE INTENTIONALLY LEFT BLANK

VI. CONCLUSIONS AND FUTURE WORK

A. CONCLUSIONS

We have considered theoretical investigations of the feasibility of parametrically exciting a mode of an acoustic resonator. The motivation of the work is that such excitation may lead to large amplitudes, which would be useful in high-amplitude resonant acoustic devices such as thermoacoustic refrigerators, acoustic pumps, and acoustic compressors. We investigated modulating the natural frequency of the fundamental mode of a straight pipe by modulating the length, and modulating the natural frequency of the fundamental radial mode of a cylindrical cavity by modulating the temperature.

For the case of modulating the length of a straight pipe, we found that it appears feasible to excite the longitudinal mode if sulfur hexafluoride is used in the resonator. The quality factor for a straight pipe filled with sulfur hexafluoride is roughly twice the value for a straight pipe filled with air. Furthermore, the relatively low sound speed of sulfur hexafluoride requires a lower drive frequency, which allows an electrodynamic driver to produce a larger displacement amplitude. For sulfur hexafluoride, we found that the Electrovoice EVX-150A driver can theoretically exceed the threshold displacement for all lengths of the resonator. If the straight pipe is filled with carbon dioxide, we found that the EVX-150A can theoretically exceed the threshold for cases where the length is greater than 1.2 meters. On the other hand, for the drivers we considered, it the threshold displacement cannot be reached for a straight pipe filled with air.

We investigated the feasibility of parametrically exciting the fundamental radial mode of a cylindrical cavity in two ways. In the first case, we considered compressing and expanding the enclosed gas and thus modulating the temperature. By assuming an ideal gas which undergoes adiabatic compressions and rarefactions, we related the change in volume to a change in temperature. We also invoked a quasistatic limit to ensure that the pressure change was approximately uniform throughout the resonator. The quasistatic limit required that the wavelength be much greater than the height of the cylindrical cavity, which forced us to consider resonators with a relatively small height. Regardless of the enclosed gas, parametric excitation of the radial mode by modulating the height was found to be infeasible for all geometries for the drivers we considered.

In the second case, we conducted a preliminary investigation into modulating the temperature using an electromagnetic wave (e.g., microwave) source. Rough calculations of the time required to conduct the heat from the resonator showed that the attainable drive frequency was three orders of magnitude *below* the required parametric drive frequency. It thus appears highly improbable that sufficient heat conduction can occur over an acoustic cycle unless the resonator is operated at extremely high temperatures.

B. FUTURE WORK

Experimental verification of the straight pipe theory contained in Chapter III appears to be the best option for future work. Our calculations show that it is very feasible to parametrically excite the fundamental longitudinal mode of a pipe containing sulfur hexafluoride. Because theoretical quality factors are generally greater than the values found in practice, the threshold value may be significantly higher, which can be

handled by arranging the drive amplitude to be much greater than the predicted threshold value. Assuming the threshold is met, such an experiment would be important in order to probe the steady state of the parametric excitation because large amplitudes may occur. It would be interesting to compare the amplitude of a parametrically excited sound wave with one produced from direct excitation. The pipe should be detuned, for example, by having a constriction or enlargement at the center, so that the second harmonic is not directly excited. In the experiment of Adler and Breazeale, the steady state apparently occurred as a result of a lack of detuning, so that the fundamental drove the second harmonic through nonlinearities. This is probably why large amplitudes did not occur.

Much of the work on the difficult problem of electromagnetic wave modulation of the temperature was cursory in order to provide a rough estimate of the feasibility. To have a sufficiently large amplitude of the temperature oscillations of a fluid such that the parametric threshold is met, there must be a relatively large time-averaged temperature difference between the maximum value in the fluid and the temperature of the walls, so that heat can quickly leave the system. Because the thermal conductivity of liquids is an order of magnitude greater than gases, liquids may prove amenable to temperature modulation. A complicating aspect is that a large temperature difference will cause convection to occur. This is advantageous because it augments the heat flow, but disadvantageous because it will lower the quality factor of the acoustic mode. A model that accounts for heat convection in addition to heat conduction may prove whether or not parametric excitation by this type of temperature modulation is possible.

THIS PAGE INTENTIONALLY LEFT BLANK

APPENDIX A. PROPERTIES OF WATER AND SELECTED GASES

Table 1 was compiled from data obtained from the CRC Handbook of Chemistry and Physics (Lide 1994), the National Institute of Standards and Technology (NIST) website, (Lemmon *et al.*, 2000), and the Thermo Chemical Calculator available on the California Institute of Technology website.

Gas	Shear Viscosity (μPa·s) μ	Density (kg/m^3) ρ	Sound speed (m/s) c	Prandtl number Pr	Ratio of specific heats γ	Constant pressure specific heat (J/kg·K) c_p	Thermal diffusivity (μm^2/s) α
Air	18.62	1.1845	346.27	0.71465	1.4017	1003.37	21.79
Ar	22.61	1.6329	321.59	0.66841	1.66667	521.56	20.69
CO_2	14.83	1.8080	268.63	0.75946	1.29417	850.76	10.99
He	19.79	0.16353	1016.4	0.68797	1.66667	5193.06	175.96
SF_6	15.33	5.9702	136.25	0.93083	1.09376	664.119	-
Water	868.40	997.05	1496.7	5.7763	1.01056	4181.3	0.1509

Table 1. Selected thermodynamic and fluid properties of water and various gases at 25° C and 1 atm.

Gas	Shear Viscosity (μPa·s) μ	Density (kg/m^3) ρ	Sound speed (m/s) c	Prandtl number Pr	Ratio of specific heats γ	Constant pressure specific heat (J/kg·K) c_p	Thermal diffusivity (μm^2/s) α
Air	18.62	2.3676	346.27	0.713	1.40082	1003.37	11.04
CO_2	-	3.6344	267.85	-	1.29990	858.17	-
He	-	0.32691	1016.8	-	1.66667	5193.06	-
SF_6	-	11.94	136.25	-	1.09376	664.119	-

Table 2. Selected thermodynamic and fluid properties of various gases at 25° C and 2 atm.

Gas	Shear Viscosity (μPa·s) μ	Density (kg/m^3) ρ	Sound speed (m/s) c	Prandtl number Pr	Ratio of specific heats γ	Constant pressure specific heat (J/kg·K) c_p	Thermal diffusivity (μm^2/s) α
Air	23.06	0.94577	386.9	0.70484	1.395	1011.3	32.71
CO_2	17.96	1.4019	297.6	0.73899	1.260	921.87	17.34

Table 3. Selected thermodynamic and fluid properties of various gases at 100° C and 1 atm.

APPENDIX B. ELECTROMECHANICAL DRIVER DISPLACEMENT

It is possible to obtain a rough estimate of the peak driver displacement by modeling an electrodynamic driver as a driven mass on a string. In general, the amplitude is

$$x_{\max} = \left| \frac{1}{j\omega} \frac{F}{R_m + j\left(\omega m - s/\omega\right)} \right|, \tag{2.1}$$

where F is the amplitude of the sinusoidal driving force, m is the driven mass, s is the stiffness constant, R_m is the mechanical resistance, and ω is the angular frequency of the drive.

In an electrodynamic loudspeaker, the radiating cone is driven by the current in a coil that moves in a constant magnetic field. The force, which produces motion of the radiating cone, is proportional to the magnetic field in the gap and the current in the coil, so the peak force is

$$F = (Bl)I, \tag{2.2}$$

where B is the magnetic field, l is the coil length, and I is the peak current in the coil. Using Ohm's Law, the peak current can be expressed as $\sqrt{2P/Z}$ where P is the rms power rating and Z is the nominal impedance of the compression driver. The factor of 2 is necessary to convert the rms power to a peak power. With this substitution, Eq. (2.2) becomes

$$F = Bl\sqrt{\frac{2P}{Z}}. \tag{2.3}$$

Using the values of the stiffness constant and the driver mass, it is possible to obtain a rough value for the maximum displacement of an electrodynamic driver. At high frequencies, the mechanical impedance approaches ωm. Thus, if the mechanical resistance is small compared to this term, then Eq. (2.1) in the *mass controlled region* approaches $F/\omega^2 m$. Similarly, at high frequencies the mechanical impedance approaches $-s/\omega$. Assuming the mechanical resistance is negligible, Eq. (2.1) in the *stiffness controlled region* approaches F/s (i.e. Hooke's Law). At resonance, the mechanical impedance vanishes and the driver amplitude reaches its maximum value of $F/\omega R_m$. Figure B.1 shows a typical resonance curve for a mass on a string as well as the approximations for the stiffness and mass controlled regions.

It is also interesting to note that the equations approximating the behavior of the piston in the mass and stiffness controlled regions intersect at the resonant frequency of the driver. This is to be expected since at resonance $\omega m = s/\omega$. Thus, the intersection of these curves must denote the resonant frequency since the mass and stiffness terms are equal.

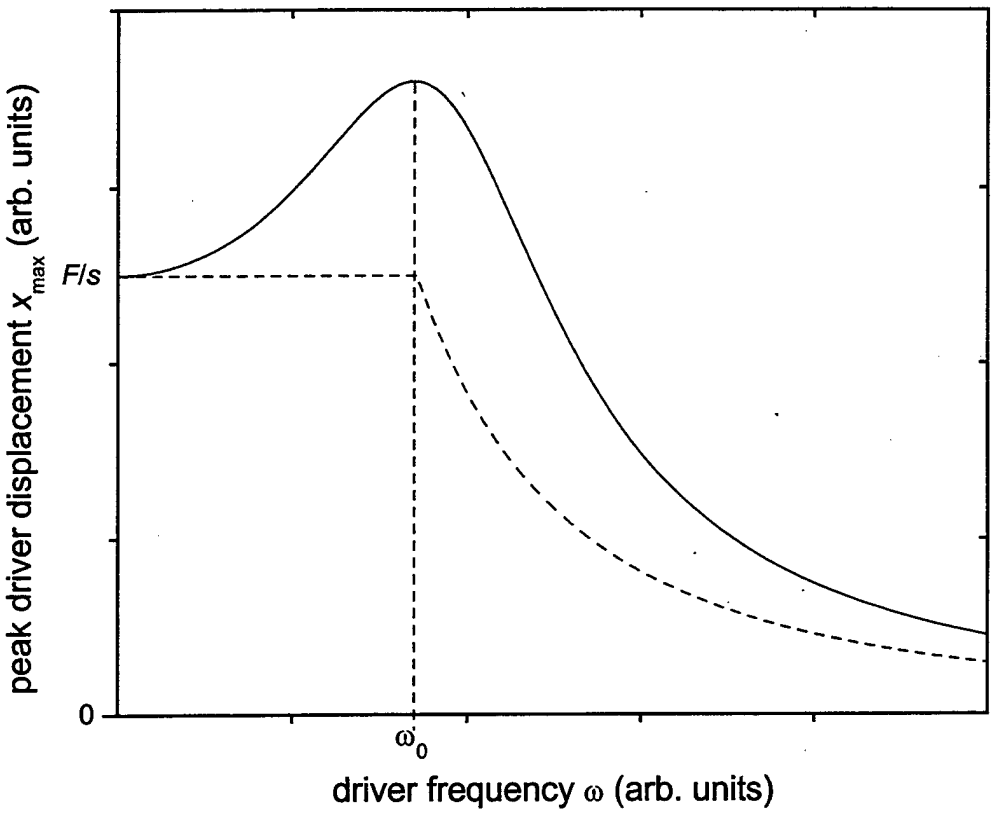

Figure B.1. Typical response of a driver compared to the behavior in the stiffness and mass controlled regions. The natural frequency is $\omega_0 = \sqrt{s/m}$.

THIS PAGE INTENTIONALLY LEFT BLANK

APPENDIX C. DRIVER SPECIFICATIONS

Table 2 lists the Thiele-Small parameters that were used to estimate the maximum displacement of a given driver. The data was compiled from technical specification sheets available from the manufacturer or from direct consultation with the manufacturer's engineers. Figures C.1 through C.6 are plots of the maximum displacement of each driver using the relationships in Appendix B and the data in Table 2.

	JBL-2490H	JBL-2450H	EVX-150A	Peerless SWR-315	ACI SV-18	Rage-12
Effective diameter (mm)	76	49	318	257	390	260
Nominal impedance (Ω)	8	6	8	8	8	8
Power Rating (W)	200	100	500	220	1000	200
Frequency range (Hz)	250-4k	500-23k	30-1.8k	-	-	-
Bl (T-m)	17	12.7	20.4	11.6	26.1	6.5
Stiffness (N/m)	47000	40800	3400	1820	3500	4310
Driver mass (g)	6.2	3.2	69	80	372	126
Free air resonance (Hz)	438	568	35.4	24	15.5	29
x_{max} (mm)	0.5 phase plug installed	0.5 phase plug installed	19.7	18	20	6.9

Table 4. Thiele-Small parameters for various drivers.

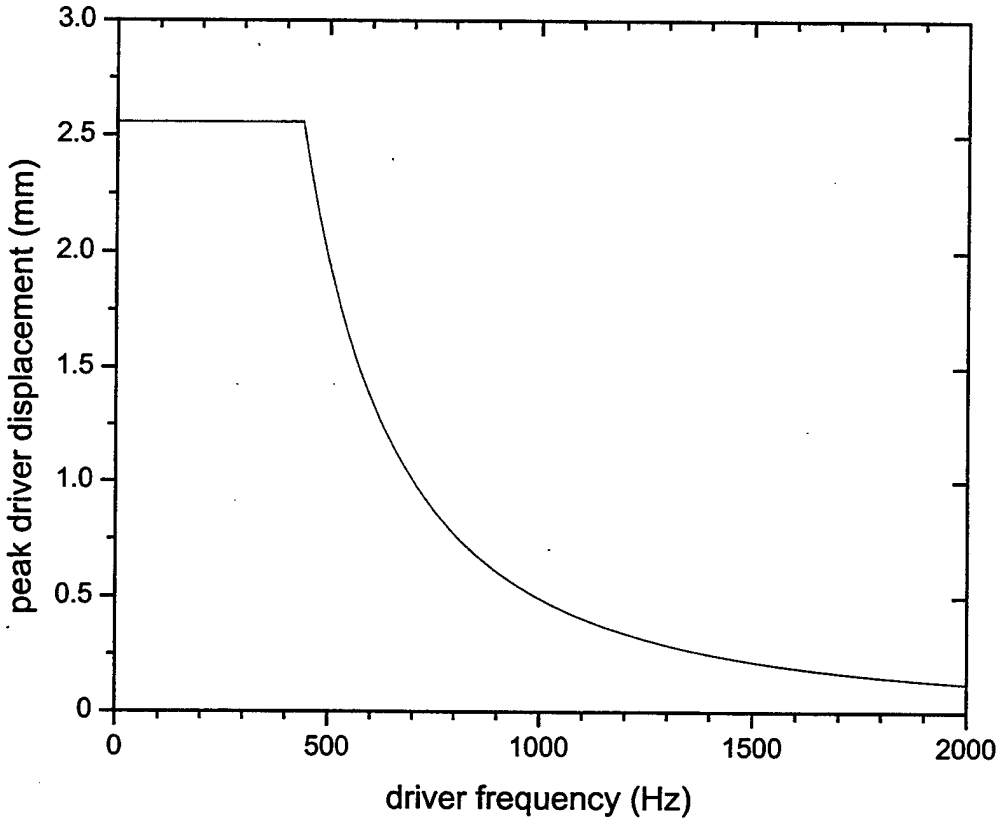

Figure C.1. Peak driver displacement for the JBL 2490H in the mass and stiffness controlled regions.

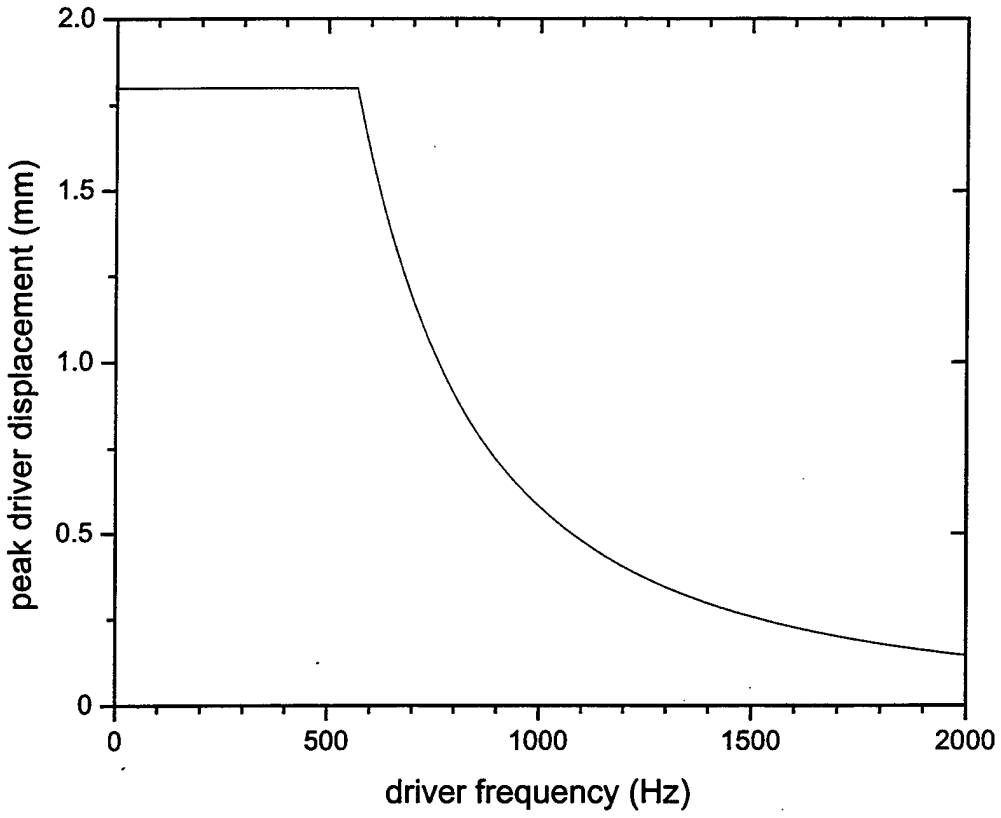

Figure C.2. JBL 2450H peak driver displacement in the mass and stiffness controlled regions.

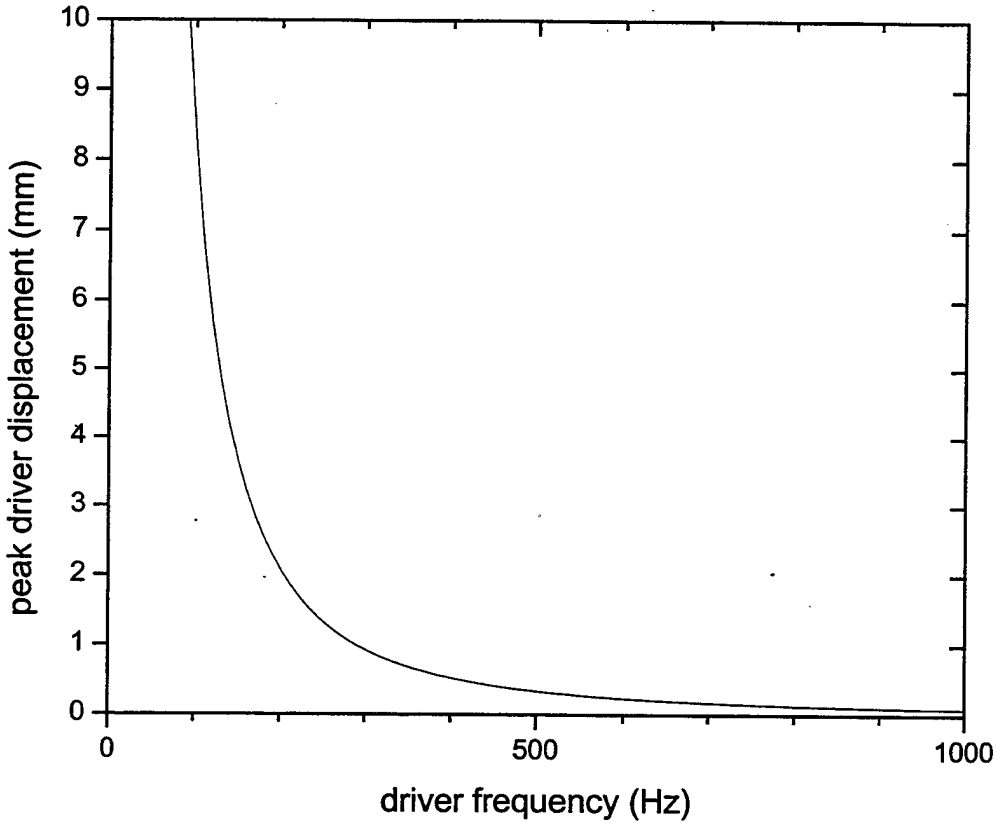

Figure C.3. EVX-150A peak driver displacement in the mass controlled region.

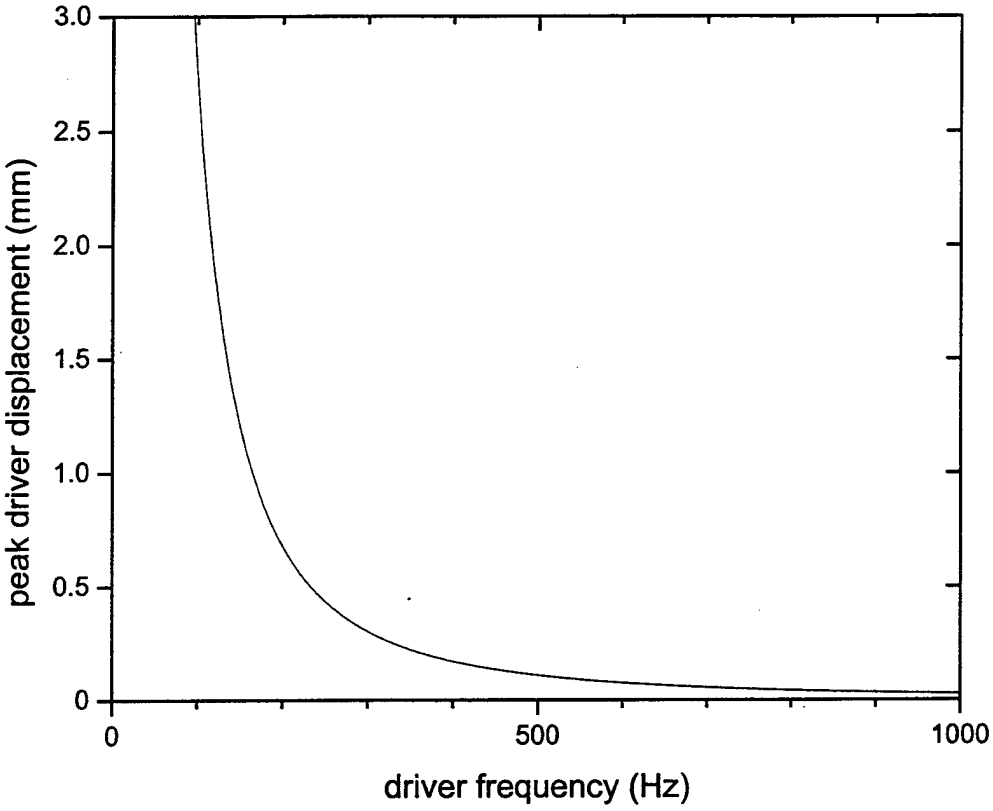

Figure C.4. SWR-315 peak driver displacement in the mass controlled region.

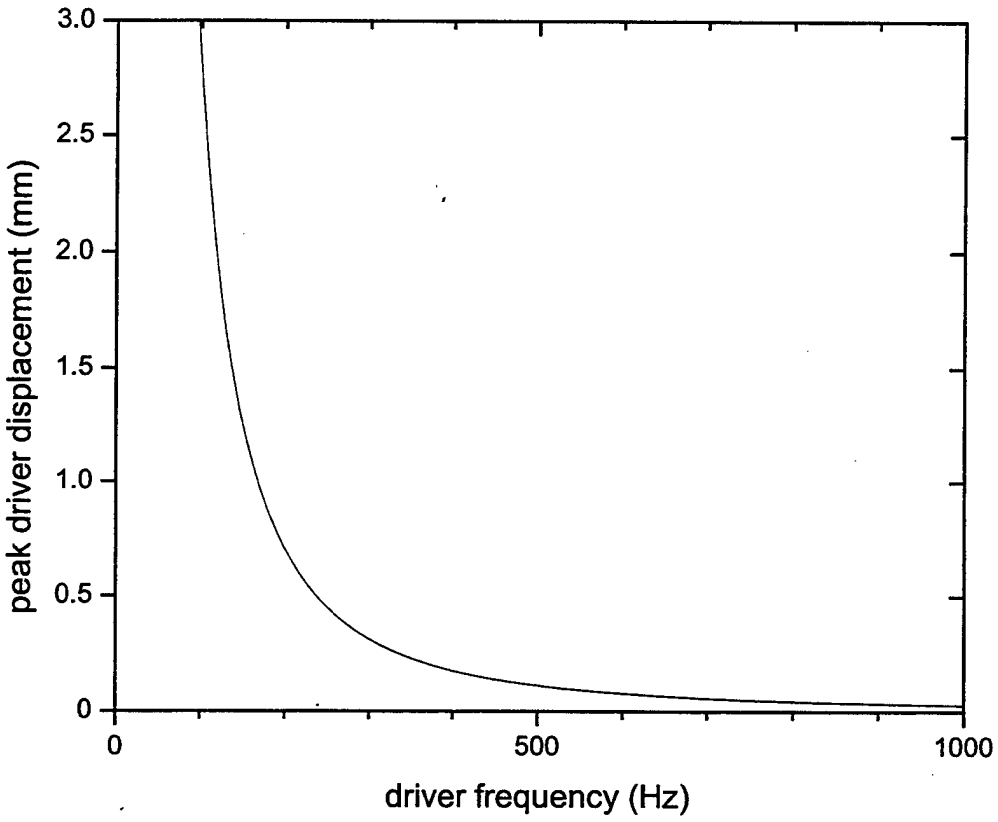

Figure C.5. SV-18 peak driver displacement in the mass controlled region.

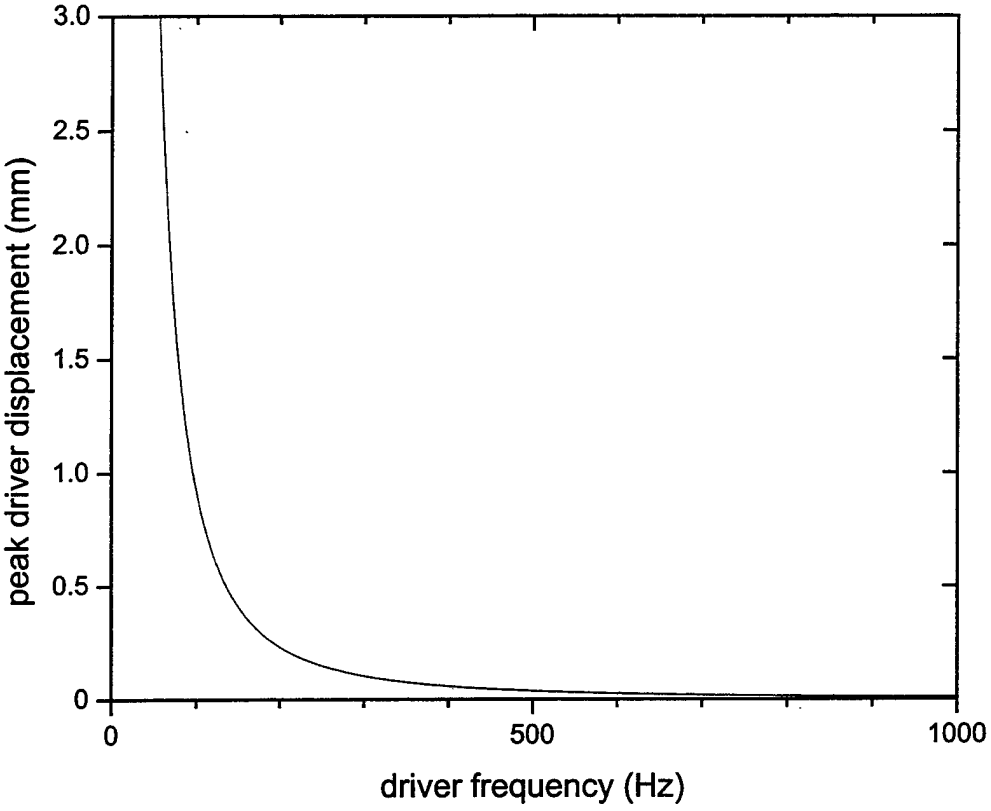

Figure C.6. Rage-12 peak driver displacement in the mass controlled region.

THIS PAGE INTENTIONALLY LEFT BLANK

APPENDIX D. VTS-100 ELECTRODYNAMIC SHAKER

In addition to the electromechanical drivers described in Appendix C, we also considered the use of an electrodynamic shaker to generate the necessary length or height modulation. The performance of the VTS-100 is shown in Figures D.1 and D.2. The maximum displacement produced by the VTS-100 is exceeded by all the other drivers compiled in Appendix C. The data contained in this appendix is provided for completeness.

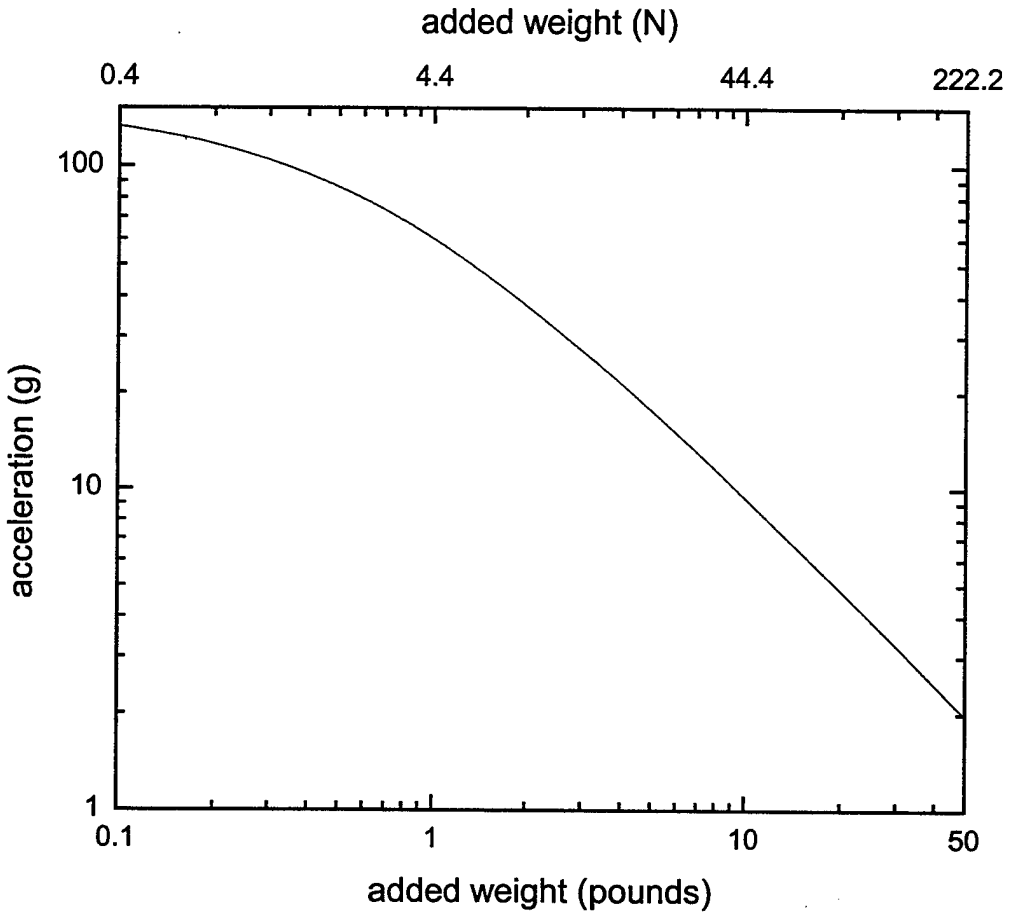

Figure D.1. Maximum acceleration produced by the VTS 100.

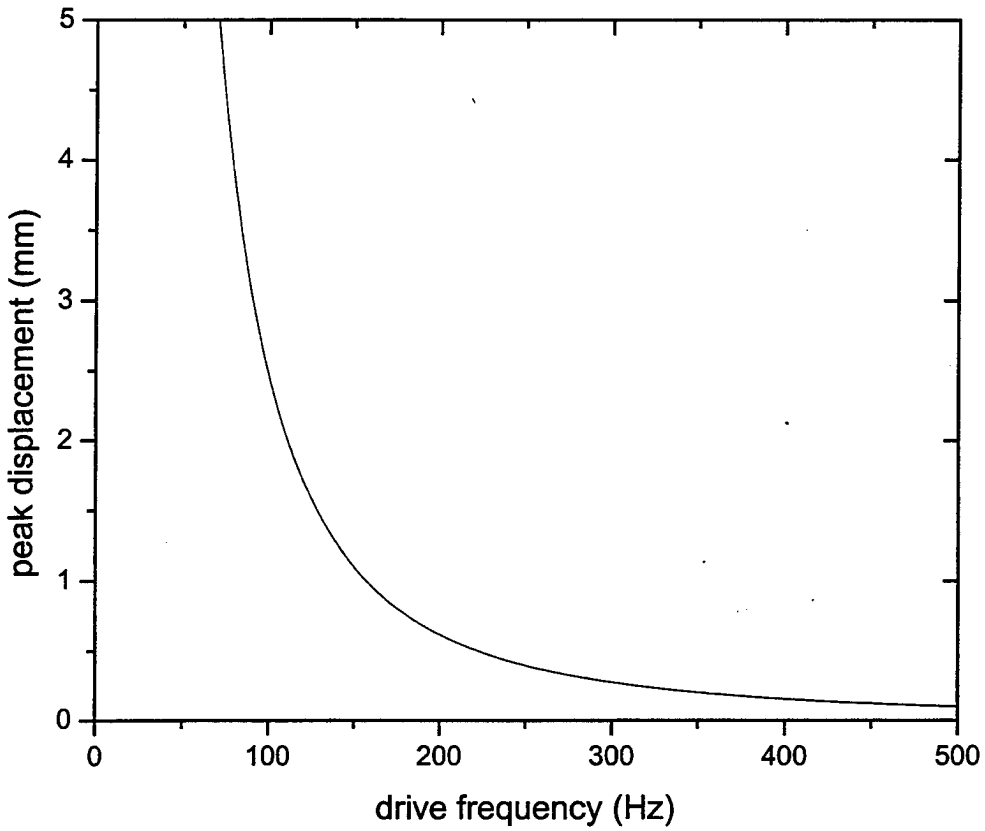

Figure D.2. Peak displacement produced by the VTS 100 with 100 g acceleration and 0.34 lbf. test load.

THIS PAGE INTENTIONALLY LEFT BLANK

LIST OF REFERENCES

Adler, L., *Parametric Generation of Ultrasonic Waves: Linear and Nonlinear Phenomena*, Ph.D. Dissertation, University of Tennessee, Knoxville, Tennessee, 1969.

Adler, L. and Breazeale, M.A., "Generation of fractional harmonics in a resonant ultrasonic wave system," *J. Acoust. Soc. Am.*, vol. 48, no. 5, pp. 1077-1083, 1970.

Blackstock, D.T., *Fundamentals of Physical Acoustics*, John Wiley & Sons, Inc., 2000.

Bogolinbov, N. and Mitropolsky, Y., *Asymptotic Methods in the Theory of Nonlinear Oscillations,* Hindustan Publishing, 1961.

Chow, T.L., *Classical Mechanics*, John Wiley & Sons, Inc., 1995.

Denardo, B. and Alkov, S., "Acoustic resonators with variable nonuniformity," *Am. J. Phys.* vol. 62, no. 4, pp. 315-321, April 1994.

Denardo, B. and Bernard, M., "Design and measurements of variably nonuniform acoustic resonators," *Am. J. Phys.* vol. 64, no. 6, pp.745-751, June 1996.

Faraday, M., "On a peculiar class of acoustical figures: and on certain forms assumed by groups of particles upon vibrating elastic surfaces," *Phil. Trans. Roy. Soc.*, pp. 299-340, 1831.

Hill, G.W., "On the part of the lunar perigee which is a function of the mean motions of the sun and moon," *Acta. Math.*, vol. 8, pp. 1-36, 1886.

Jackson, J.D., *Classical Electrodynamics*, John Wiley & Sons, Inc., 1975.

Kinsler, L.E., Frey, A.R., Coppens, A.B., and Sanders, J.V., *Fundamentals of Acoustics*, John Wiley & Sons, Inc., 2000.

Lamb, Clifford, private communication, 2000.

Landau, L.D. and Lifshitz, E.M. *Fluid Mechanics*, Pergamon, 1959.

Lemmon, E.W., McLinden M.O., and Friend D.G., "Thermophysical Properties of Fluid Systems" in NIST Chemistry WebBook, NIST Standard Reference Database Number 69, Eds. W.G. Mallard and P.J. Linstrom, February 2000, National Institute of Standards and Technology, Gaithersburg MD, 20899 (http://webbook.nist.gov).

Lide, David R., *CRC Handbook of Chemistry and Physics*, 75th ed., CRC Press, 1994.

Mandelstam, L., and others, "Expose des recherches recentes sur les oscillations non lineaires," *Tech. Phys. USSR,* vol. 2, no. 81, 1935.

Melde, F., "Uber erregung stehender wellen eines fadenformigen korpers," *Ann. Phys. Chem.*, vol. 109, pp. 193-215, 1859.

Pinto, Fabrizio, "Parametric resonance: an introductory experiment," *The Physics Teacher*, vol. 31, pp. 336-346, September 1993.

Powers, D. L., *Boundary Value Problems,* Harcourt Brace Jovanovich, Inc., 1987.

Prather, Wayne E., *Parametric excitation of a resonant acoustic mode*, Ph.D. Dissertation, University of Mississippi, University, Mississippi, August 1999.

Raspet, R., Denardo, B., Bass, H.E., Brewaster, J. and Kordomenos, J., "Investigation of parametric drive of a longitudinal gas-filled resonance tube," *J. Acoust. Soc. Am.*, vol. 99, no. 2, pp. 725-729, February 1996.

Rayleigh, Lord, "On maintained vibrations," *Phil. Mag.*, April 1883.

Rayleigh, Lord, "On the maintenance of vibrations by forces of double frequency, and on the propagation of waves through a medium endowed with a periodic structure," *Phil. Mag.*, August 1887.

Swift, G.W., "Thermoacoustic engines," *J. Acoust. Soc. Am.*, vol. 84, no. 4, pp. 1145-1180, October 1988.

Wright, W.B. and Swift, G.W., "Parametrically driven variable-reluctance generator," *J. Acoust. Soc. Am.*, vol. 88, no. 2, pp. 609-615, August 1990.

INITIAL DISTRIBUTION LIST

1. Defense Technical Information Center 2
   8725 John J. Kingman Road, Suite 0944
   Ft. Belvoir, VA 22060-6218

2. Dudley Knox Library 2
   Naval Postgraduate School
   411 Dyer Road
   Monterey, CA 93943-5101

3. Physics Department 2
   Naval Postgraduate School
   833 Dyer Road
   Monterey, CA 93943-5002

4. Engineering & Technology Curricular Office, Code 34 1
   411 Dyer Road
   Naval Postgraduate School
   Monterey, CA 93943-5101

5. Professor Bruce Denardo 5
   Department of Physics
   Naval Postgraduate School
   Monterey, CA 93943-5002

6. Professor Thomas Hofler 1
   Department of Physics
   Naval Postgraduate School
   Monterey, CA 93943-5002

7. Naval Submarine School 2
   Code N222 SOAC 01050
   P.O. Box 700
   ATTN: LT Larry P. Varnadore
   Groton, CT 06349-5700